J. Numer. Math. 2025; aop

Duk-Soon Oh* and Shangyou Zhang

New analysis of overlapping Schwarz methods for vector field problems in three dimensions with generally shaped domains

https://doi.org/10.1515/jnma-2024-0080 Received May 30, 2024; accepted June 13, 2025; published online September 9, 2025

Abstract: This paper introduces a novel approach to analyze two-level overlapping Schwarz methods for Nédélec and Raviart—Thomas vector field problems. The theory is based on new regular stable decompositions for vector fields that are robust to the topology of the domain. Enhanced estimates for the condition numbers of the preconditioned linear systems are derived, dependent linearly on the relative overlap between the overlapping subdomains. Furthermore, we present the numerical experiments which support our theoretical results.

Keywords: overlapping Schwarz; H(curl); Nédélec finite element; H(div); Raviart–Thomas finite element

MSC 2010 Classification: 65N55; 65N30; 65F08; 65F10

1 Introduction

Let Ω be a bounded Lipschitz domain in \mathbb{R}^3 . We assume that the domain Ω is scaled such that the diameter of Ω is equal to one. We first introduce the Hilbert space $H(\mathbf{curl}; \Omega)$ that consists of square integrable vector fields on the domain Ω that have square integrable curls. We consider the following model problem posed in $H(\mathbf{curl}; \Omega)$: Find $u \in H(\mathbf{curl}; \Omega)$ such that

$$a_c(\mathbf{u}, \mathbf{v}) = (\mathbf{f}, \mathbf{v}) \quad \forall \mathbf{v} \in H(\mathbf{curl}; \Omega),$$
 (1)

where

$$a_c(\mathbf{u}, \mathbf{v}) := \eta_c(\mathbf{curl}\,\mathbf{u}, \mathbf{curl}\,\mathbf{v}) + (\mathbf{u}, \mathbf{v}) \tag{2}$$

and (\cdot, \cdot) is the standard inner product on $(L^2(\Omega))^3$ or $L^2(\Omega)$. We assume that the constant η_c is positive and $\mathbf{f} \in (L^2(\Omega))^3$. We also consider the Hilbert space $H(\operatorname{div}; \Omega)$ in a similar manner, i.e., the space of square integrable vector fields on Ω with square integrable divergences. The corresponding model problem for a square integrable vector field $\mathbf{g} \in (L^2(\Omega))^3$ on Ω is given as follows: Find $\mathbf{p} \in H(\operatorname{div}; \Omega)$ such that

$$a_d(\mathbf{p}, \mathbf{q}) = (\mathbf{g}, \mathbf{q}) \quad \forall \mathbf{q} \in H(\text{div}; \Omega),$$
 (3)

where

$$a_d(\mathbf{p}, \mathbf{q}) := \eta_d(\operatorname{div} \mathbf{p}, \operatorname{div} \mathbf{q}) + (\mathbf{p}, \mathbf{q}). \tag{4}$$

Similarly, we assume that η_d is a positive constant.

^{*}Corresponding author: Duk-Soon Oh, Department of Mathematics, Chungnam National University, Daejeon, Republic of Korea, E-mail: duksoon@cnu.ac.kr. https://orcid.org/0000-0002-6583-0967

Shangyou Zhang, Department of Mathematical Sciences, University of Delaware, Newark, DE 19716, USA, E-mail: szhang@udel.edu. https://orcid.org/0000-0002-1114-4179

Open Access. © 2025 the author(s), published by De Gruyter. This work is licensed under the Creative Commons Attribution 4.0 International License.

The first model problem (1) is originated from time-dependent Maxwell's equation, specifically the eddycurrent problem; see [1], [2]. With a suitable time discretization, we have to solve the problem (1) in each time step. The second problem (3) is developed for a first-order system of least-squares formulation for standard second order elliptic problems. For more detail, see [3]. We also note that efficient numerical solution methods related to (3) are required for solving problems from a pseudostress-velocity formulation for the Stokes equations and a sequential regularization method for the Navier-Stokes equations; see [4], [5].

A number of attempts have been made to develop domain decomposition methods for solving (1) and (3). In [6]-[9], overlapping Schwarz methods applied to (1) have been considered. Additionally, nonoverlapping domain decomposition methods have been introduced in [10]-[12]. In regard to the model problem (3), both overlapping and nonoverlapping domain decomposition methods have been proposed in the literature. The former can be found in [7], [8], [13], [14], while the latter can be found in [15], [16]. However, there are topological constraints associated with the domains or subdomains; see [7]-[9], [13]-[15]. To be more precise, the theories in [7]-[9], [13] are based on the assumption that the domain is convex, while the convexity of subdomains is assumed to establish the results in [14], [15]. In recent constructions [6], [12] novel algorithms have been proposed to handle irregularly shaped subdomains. However, no supporting theories have yet been formulated. Finally, the theoretical results presented in [7], [9]-[11], [14], [16] are not sharp. Specifically, the results in [10], [11], [16] depend on the material parameters used in the model problems, while the results in [7], [9], [11], [14] include additional factors not present in the numerical experiments. This paper proposes a new theory that addresses the shortcomings of the aforementioned references.

The framework for analyzing domain decomposition methods based on overlapping subdomains has been introduced in [17] as a subspace correction method. The two-level overlapping Schwarz methods for scalar elliptic problems have been introduced and analyzed in [18]; see also [19, Sect. 3] and references therein for more detailed techniques. In [18], it is proved that the condition number of the preconditioned linear system is bounded above by a constant multiple of $(1 + H/\delta)$, where H is the diameter of the subdomain and δ is the size of the overlap between subdomains. In fact, the bound is shown to be optimal; see [20].

The purpose of this paper is to analyze two-level overlapping Schwarz methods for discretized problems originated from (1) and (3) using appropriate finite elements, i.e., Nédélec and Raviart-Thomas elements of the lowest order. Such methods have been first introduced and analyzed in [7], [9]. Historically, the authors in [7], [9] proved an upper bound $(1 + H^2/\delta^2)$ for the $H(\mathbf{curl})$ and $H(\mathbf{div})$ finite elements. They conjectured and numerically tested that the best upper bound is $(1 + H/\delta)$. This conjecture was numerically checked many times by others. After twenty-three years, the open problem was solved by [8] with the best upper bound $(1 + H/\delta)$ being proved. In this paper, we prove again the best upper bound $(1 + H/\delta)$ without the H^1 -regularity assumption used by [8] That is, we allow nonconvex domains and non-simply-connect domains.

Previously, the first author of this paper proved an improved bound, $(1 + \log(H/h))(1 + H/\delta)$ versus $(1 + H^2/\delta^2)$, in [14] with a nonstandard coarse space method assuming that subdomains are convex, where h is the size of the mesh for the finite elements. In this paper, we do not have any assumptions related to the topological properties of the domain and subdomains. These properties may encompass nonconvex geometries, potentially accompanied by holes. Consequently, our results offer insight into closely related practical applications, such as, in magnetohydrodynamics, a field in which simulating on a torus-like domain is of significant importance. We remark that the algorithms in [7]-[9] and this paper are essentially the same but the technical details for the theories are different.

The important ingredients for analyzing numerical methods for solving problems posed in $H(\mathbf{curl})$ and H(div) are the Helmholtz type decompositions. This is because the structures of the kernels of the curl and the divergence operators are quite different from that of the gradient operator. In [7], [9], discrete orthogonal Helmholtz decompositions based on those for continuous spaces have been suggested and used for analyzing overlapping Schwarz methods. Since the discrete range spaces are not included in the continuous range spaces, the authors had to introduce semi-continuous spaces to handle the difficulty. To do so, the convexity of the domain was needed to use a suitable embedding. In [8], the authors considered the same type of decompositions so that the assumption for the domain has been inherited. In this paper, we consider a different type of regular

decompositions. By introducing an additional term, an oscillatory component, and abandoning the orthogonality, we have more robust decompositions, cf. (10) and (11). The approaches have been originally introduced in [21] and extended later in [22]–[24] based on the cochain projections constructed in [25]. Our theories will be based on the decompositions suggested by Hiptmair and Pechstein; see [22]-[24].

The rest of the paper is organized as follows. In Section 2, we introduce the discrete model problems and related finite elements. We describe overlapping Schwarz preconditioners in Section 3. We next provide our theoretical results in Section 4. Finally, the numerical examples to support our theories are presented in Section 5.

2 The discrete problems

We consider two triangulations, \mathcal{T}_H and \mathcal{T}_h . First, we introduce \mathcal{T}_H , a coarse triangulation of the domain Ω , consisting of shape-regular and quasi-uniform tetrahedral elements with a maximum diameter H. Subsequently, \mathcal{T}_h is generated as a finer mesh, a refinement of the coarse mesh \mathcal{T}_H . It is assumed that the restriction of \mathcal{T}_h to each individual coarse element is both shape-regular and quasi-uniform.

We next introduce finite element spaces. The space of the lowest order tetrahedral Nédélec finite elements associated with $H(\mathbf{curl}; \Omega)$ and the triangulation \mathcal{T}_h is defined by

$$\mathcal{ND}_h := \{ \boldsymbol{u} \mid \boldsymbol{u}_{|K} \in N(K), K \in \mathcal{T}_h \text{ and } \boldsymbol{u} \in H(\mathbf{curl}; \Omega) \},$$

where the set of the shape functions N(K) is given by

$$N(K) := \{ \alpha_c + \beta_c \times x \mid \alpha_c \text{ and } \beta_c \text{ are constant vectors in } \mathbb{R}^3 \}$$
 (5)

for a tetrahedral element. We note that the values of two vectors $\boldsymbol{\alpha}_c$ and $\boldsymbol{\beta}_c$ in (5) can be determined by the average tangential components on the edges of K, i.e.,

$$\lambda_e^{\mathcal{N}D}(\mathbf{u}) := \frac{1}{|e|} \int \mathbf{u} \cdot \mathbf{t}_e \mathrm{d}s, \quad e \subset \partial K,$$

where |e| is the length of the edge e and t_e is the unit tangential vector associated with e. We note that these values can be considered as the degrees of freedom. The interpolation operator $\Pi_h^{\mathcal{N}D}$ for a sufficiently smooth vector field ${\it u}$ in ${\it H}({\it curl};~\Omega)$ onto ${\it ND}_h$ is defined as follows:

$$\Pi_h^{\mathcal{N}D} \boldsymbol{u} := \sum_{e \in \mathcal{E}_h} \lambda_e^{\mathcal{N}D}(\boldsymbol{u}) \, \Phi_e^{\mathcal{N}D},$$

where \mathcal{E}_h is the set of interior edges of \mathcal{T}_h and $\Phi_e^{\mathcal{N}\mathcal{D}}$ is the standard basis function linked with e, i.e., $\lambda_e^{\mathcal{N}D}(\Phi_e^{\mathcal{N}D}) = 1 \text{ and } \lambda_{e'}^{\mathcal{N}D}(\Phi_e^{\mathcal{N}D}) = 0 \text{ for } e' \neq e.$

Remark 1. In general, the interpolation operator $\Pi_h^{\mathcal{N}D}$ is not well defined in the entire space $H(\mathbf{curl}; \Omega)$. This is because additional regularity, e.g., **curl** $u \in (L^p(K))^3$ and $u \times n \in (L^p(\partial K))^3$ for p > 2 and $K \in \mathcal{T}_h$, is needed to define and the tangential component for $u \in H(\mathbf{curl}; \Omega)$, where n is the outward unit normal vector.

We next consider the lowest order tetrahedral Raviart-Thomas finite element space corresponding to the space $H(\text{div}; \Omega)$ that is defined by

$$\mathcal{RT}_h := \{ p \mid p_{|K} \in R(K), K \in \mathcal{T}_h \text{ and } p \in H(\text{div}; \Omega) \}.$$

Here, the set of shape functions R(K) associated with the tetrahedral element K is defined by

$$R(K) := \{ \alpha_d + \beta_d x \mid \alpha_d \text{ is a constant vector in } \mathbb{R}^3 \text{ and } \beta_d \text{ is a scalar} \}.$$

The degrees of freedom related to an element *K* are determined by the average values of the normal components over its faces, namely

$$\lambda_f^{\mathcal{RT}}(\boldsymbol{p}) := \frac{1}{|f|} \int_f \boldsymbol{p} \cdot \boldsymbol{n}_f \mathrm{d}s, \quad f \subset \partial K.$$

Here, |f| is the area of the face f and \mathbf{n}_f is the unit normal vector corresponding to f. We note that $\boldsymbol{\alpha}_d$ and $\boldsymbol{\beta}_d$ can be completely recovered by the degrees of freedom associated with the four faces of K. Let \mathcal{F}_h be the set of interior faces of \mathcal{T}_h . Similarly, we can define the interpolation operator $\Pi_h^{\mathcal{RT}}$ associated with $H(\operatorname{div}; \Omega)$. For a sufficiently smooth $\boldsymbol{p} \in H(\operatorname{div}; \Omega)$, the operator is defined by

$$\Pi_h^{\mathcal{R}\mathcal{T}} \boldsymbol{p} := \sum_{f \in \mathcal{F}_h} \lambda_f^{\mathcal{R}\mathcal{T}}(\boldsymbol{p}) \, \Phi_f^{\mathcal{R}\mathcal{T}}.$$

Here, $\Phi_f^{\mathcal{RT}}$ is the standard basis function corresponding to the face f, i.e., $\lambda_f^{\mathcal{RT}}(\Phi_f^{\mathcal{RT}}) = 1$ and $\lambda_{f'}^{\mathcal{RT}}(\Phi_f^{\mathcal{RT}}) = 0$ for $f' \neq f$.

Remark 2. Like the interpolation operator for edge elements, the normal component on the face must be well defined to introduce the interpolation $\Pi_h^{\mathcal{R}\mathcal{T}}$. Thus, some additional regularity for $p \in H(\text{div}; \Omega)$ is required, e.g., $p \in (H^r(\Omega))^3$ for r > 1/2.

In addition, we need the piecewise linear space for our theories. Let S_h be the space of the continuous P_1 finite elements associated with \mathcal{T}_h . We recall that the degrees of freedom are given by the function evaluations at the vertices. The corresponding interpolation operator for a sufficiently smooth function in $H^1(\Omega)$ is given by Π_h^S . We also consider $\widetilde{\Pi}_h^S$, the Scott–Zhang interpolation operator introduced in [26]. We can also consider the interpolation operators for \mathcal{T}_H by replacing the subscript with H. We finally define the vector field finite space $(S_h)^3$ in three dimensions, whose components are contained in S_h .

By restricting the model problems (1) and (3) to the finite element spaces \mathcal{ND}_h and \mathcal{RT}_h , respectively, we obtain the following discrete problems: Find $\mathbf{u}_h \in \mathcal{ND}_h$ such that

$$a_c(\boldsymbol{u}_h, \boldsymbol{v}_h) = (\boldsymbol{f}, \boldsymbol{v}_h) \quad \forall \boldsymbol{v}_h \in \mathcal{N}D_h$$

and find $p_h \in \mathcal{RT}_h$ such that

$$a_d(\boldsymbol{p}_h, \boldsymbol{q}_h) = (\boldsymbol{g}, \boldsymbol{q}_h) \quad \forall \boldsymbol{q}_h \in \mathcal{RT}_h.$$

We also define the operators $A_c: \mathcal{N}D_h \to \mathcal{N}D_h$ and $A_d: \mathcal{RT}_h \to \mathcal{RT}_h$ as follows:

$$(A_c \mathbf{u}_h, \mathbf{v}_h) = a_c(\mathbf{u}_h, \mathbf{v}_h) \quad \forall \mathbf{u}_h, \mathbf{v}_h \in \mathcal{N}\mathcal{D}_h$$

and

$$(A_d \boldsymbol{p}_h, \boldsymbol{q}_h) = a_d(\boldsymbol{p}_h, \boldsymbol{q}_h) \quad \forall \boldsymbol{p}_h, \boldsymbol{q}_h \in \mathcal{RT}_h.$$

3 Overlapping Schwarz methods

We decompose the domain Ω into N nonoverlapping subdomains Ω_i , a union of a few elements in \mathcal{T}_H . We assume that the number of coarse elements contained in each subdomain is uniformly bounded. The parameter H_i is defined by the diameter of the subdomain Ω_i . We now consider an overlapping subdomain Ω_i' originated from the nonoverlapping subdomain Ω_i by extending layers of fine elements, i.e., Ω_i' containing Ω_i is a union of fine elements. In addition, we consider the assumptions introduced in [19, Assumptions 3.1, 3.2, and 3.5].

Assumption 1. For $i=1,2,\ldots,N$, there exists $\delta_i>0$, such that, if x belongs to Ω_i' , then

$$\operatorname{dist}(x, \partial \Omega_j' \backslash \partial \Omega) \geqslant \delta_i \tag{6}$$

for a suitable index j = j(x), possibly equal to i and may depend on x, with $x \in \Omega'_i$.

Assumption 1 states that the overlap parameters δ_i , $i=1,\ldots,N$, represent the width of the extended regions $\Omega'_i \setminus \Omega_i$.

Assumption 2. The partition $\{\Omega'_i\}$ can be colored using at most N_0 colors, in such a way that subregions with the same color are disjoint.

Based on Assumption 2, every point $x \in \Omega$ belongs at most N_0 overlapping subdomains.

Assumption 3. There exists a constant C independent of \mathcal{T}_H and the subdomain Ω'_i , such that, for $i=1,2,\ldots,N$,

$$H_K \leqslant CH_i$$
 (7)

for any $K \in \mathcal{T}_H$, such that $K \cap \Omega'_i \neq \emptyset$. Here, H_K is the diameter of the coarse element K.

According to Assumption 3, the size of a coarse element should not be large compared to the size of the overlapping subdomains that it intersects.

The aforementioned three assumptions play critical roles in both theoretical and computational aspects. From a theoretical perspective, the parameters δ_i , H_i , and N_0 are incorporated into the estimations of the condition numbers of the preconditioned linear systems, which will be presented in Section 4. Consequently, these assumptions can serve as effective guidelines for computational settings.

In our theories, a partition of unity technique plays an essential role. To do so, we construct the set $\{\theta_i\}_{i=1}^n$ consisting of piecewise linear functions associated with the overlapping subdomain, which has the following properties:

$$0 \leq \theta_{i} \leq 1,$$

$$\operatorname{supp}(\theta_{i}) \subset \overline{\Omega'_{i}},$$

$$\sum_{i=1}^{N} \theta_{i} \equiv 1, \quad \mathbf{x} \in \Omega,$$

$$\|\nabla \theta_{i}\|_{\infty} \leq \frac{C}{\delta_{i}},$$
(8)

where C is a constant independent of the δ_i and the H_i and $\|\cdot\|_{\infty}$ is the standard L^{∞} -norm. For more details, see [19, Lem. 3.4].

We now construct our preconditioners based on overlapping Schwarz methods. We first consider the coarse component. The coarse operators $A_c^{(0)}$ and $A_d^{(0)}$ related to the coarse problems are defined as follows:

$$\left(A_c^{(0)} \boldsymbol{u}_H, \boldsymbol{v}_H\right) = a_c \left(\boldsymbol{u}_H, \boldsymbol{v}_H\right) \quad \forall \boldsymbol{u}_H, \boldsymbol{v}_H \in \mathcal{N}\mathcal{D}_H$$

and

$$\left(A_d^{(0)} \boldsymbol{p}_H, \boldsymbol{q}_H\right) = a_d(\boldsymbol{p}_H, \boldsymbol{q}_H) \quad \forall \boldsymbol{p}_H, \boldsymbol{q}_H \in \mathcal{RT}_H.$$

The row entries of the operator $R_c^{(0)}$ which maps a vector field in $\mathcal{N}\mathcal{D}_h$ to $\mathcal{N}\mathcal{D}_H$ consist of the coefficients obtained through the interpolation of the standard basis functions associated with $\mathcal{N}\mathcal{D}_H$ onto the mesh \mathcal{T}_h . We remark that $R_c^{(0)^T}: \mathcal{N}\mathcal{D}_H \to \mathcal{N}\mathcal{D}_h$ is the natural injection since the finite element spaces are nested. In a similar way, we can define the operator $R_d^{(0)}: \mathcal{RT}_h \to \mathcal{RT}_H$ associated with the Raviart–Thomas spaces. Regarding the local components, let us define the restriction operators $R_c^{(i)}: \mathcal{ND}_h \to \mathcal{ND}_h^{(i)}$ in such a way

that $R_c^{(i)T}: \mathcal{N}\mathcal{D}_h^{(i)} \to \mathcal{N}\mathcal{D}_h$ are natural injections. Here, $\mathcal{N}\mathcal{D}_h^{(i)}$ is the subspace of $\mathcal{N}\mathcal{D}_h$ spanned by the basis functions corresponding to the fine edges in Ω_i' . Similarly, the construction for $R_d^{(i)}: \mathcal{RT}_h \to \mathcal{RT}_h^{(i)}$ is straightforward, where the local space $\mathcal{RT}_h^{(i)}$ is defined in a similar way. Then, the local operators $A_c^{(i)}$ and $A_d^{(i)}$ can be defined as follows:

$$A_{\xi}^{(i)} = R_{\xi}^{(i)} A_{\xi} R_{\xi}^{(i)^{T}}, \quad 1 \leq i \leq N,$$

where ξ corresponds c or d. We note that $A_{\xi}^{(i)}$ is just a principal minor of A_{ξ} .

We can now construct the preconditioners and the resulting preconditioned linear operator has the following form:

$$M_{\xi}^{-1} A_{\xi} = \sum_{i=0}^{N} R_{\xi}^{(i)^{T}} A_{\xi}^{(i)-1} R_{\xi}^{(i)} A_{\xi}, \tag{9}$$

where ξ corresponds c or d.

4 Condition number estimate

4.1 Preliminaries

In this subsection, we will describe several preliminary results for our theories.

We first consider standard Sobolev spaces and their norms and semi-norms. For any $\mathcal{D} \subset \Omega$, let us denote by $\|\cdot\|_{s,\mathcal{D}}$ and $\|\cdot\|_{s,\mathcal{D}}$ the norm and the semi-norm of the Sobolev space $H^s(\mathcal{D})$, respectively. Provided that $\mathcal{D} = \Omega$, we will omit the subscript Ω for convenience. If there is no explicit confusion, the same norm and semi-norm notations will be used for $(H^s(\mathcal{D}))^3$.

We next define the operator $Q_H^{\mathcal{N}D}$: $(L^2(\Omega))^3 \to \mathcal{N}\mathcal{D}_H$ as the L^2 -projection onto $\mathcal{N}\mathcal{D}_H$. Similarly, we define the L^2 -projection operator $Q_H^{\mathcal{R}\mathcal{T}}$: $(L^2(\Omega))^3 \to \mathcal{R}\mathcal{T}_H$. We then have the following lemma in [19, Ch. 10].

Lemma 1. For $u, p \in (H^1(\Omega))^3$, the following estimates hold:

$$\begin{split} \left\| \mathbf{curl} \left(Q_H^{\mathcal{N}D} \boldsymbol{u} \right) \right\|_0 & \leq C |\boldsymbol{u}|_1, \\ \left\| \boldsymbol{u} - Q_H^{\mathcal{N}D} \boldsymbol{u} \right\|_0 & \leq C H |\boldsymbol{u}|_1, \\ \left\| \mathrm{div} \left(Q_H^{\mathcal{R}T} \boldsymbol{p} \right) \right\|_0 & \leq C |\boldsymbol{p}|_1, \\ \left\| \boldsymbol{p} - Q_H^{\mathcal{R}T} \boldsymbol{p} \right\|_0 & \leq C H |\boldsymbol{p}|_1 \end{split}$$

with constants independent of \mathbf{u} , \mathbf{p} , and H.

We also denote by $Q_{H,K}^0$: $(L^2(K))^3 \to (P_0(K))^3$, where $K \in \mathcal{T}_H$ and $P_0(K)$ is the space of constants, a local L^2 -projection operator. Then, we have the following result.

Lemma 2. Let $K \in \mathcal{T}_H$. Then, for $\mathbf{u} \in (H^1(K))^3$, we have

$$\left\| \boldsymbol{u} - Q_{H,K}^{0} \boldsymbol{u} \right\|_{0,K} \leqslant C H_{K} |\boldsymbol{u}|_{1,K},$$

where H_K is the diameter of K.

The following lemma describes the stability of the interpolation operators, stated in [19, Ch. 10], for the functions obtained by the product of a piecewise linear function and a vector field.

Lemma 3. Let $\mathbf{u} \in \mathcal{ND}_h$, $\mathbf{p} \in \mathcal{RT}_h$, and ϑ_i be any continuous, piecewise linear function supported in the subdomain Ω'_i . Then, we have the following estimates:

$$\begin{split} \left\| \Pi_h^{\mathcal{N}D} (\boldsymbol{\vartheta}_i \boldsymbol{u}) \right\|_{0,\Omega_i'} & \leq C \|\boldsymbol{\vartheta}_i \boldsymbol{u}\|_{0,\Omega_i'}, \\ \left\| \mathbf{curl} \left(\Pi_h^{\mathcal{N}D} (\boldsymbol{\vartheta}_i \boldsymbol{u}) \right) \right\|_{0,\Omega_i'} & \leq C \left\| \mathbf{curl} \left(\boldsymbol{\vartheta}_i \boldsymbol{u} \right) \right\|_{0,\Omega_i'}, \\ \left\| \Pi_h^{\mathcal{R}T} (\boldsymbol{\vartheta}_i \boldsymbol{p}) \right\|_{0,\Omega_i'} & \leq C \|\boldsymbol{\vartheta}_i \boldsymbol{p}\|_{0,\Omega_i'}, \end{split}$$

$$\left\|\operatorname{div}\left(\Pi_{h}^{\mathcal{RT}}(\vartheta_{i}\boldsymbol{p})\right)\right\|_{0,\Omega_{i}'} \leq C \left\|\operatorname{div}\left(\vartheta_{i}\boldsymbol{p}\right)\right\|_{0,\Omega_{i}'}.$$

In order to analyze overlapping Schwarz methods, it is necessary to find an appropriate estimate for functions on the layer surrounding the subdomain Ω_i . In [19, Lem. 3.10], an estimate for H^1 functions has been proposed. Subsequently, this estimate has been extended to include piecewise H^1 functions in [8, Lem. 3.3], on the condition that the subdomain $\Omega_i \in \mathcal{T}_H$. We note that the estimate is equally valid with assumptions in the beginning of Section 3 together with Assumptions 1, 2 and 3. We will now proceed to introduce the aforementioned

Prior to this, we will define the region $\Omega_{i\delta}$ by

$$\Omega_{i,\delta} = \bigcup_{\substack{j \in I_i \\ j \neq i}} \Omega_i' \cap \Omega_j',$$

where $I_i = \{j: \Omega'_i \cap \Omega'_i \neq \emptyset\}.$

Lemma 4. Let u be a piecewise H^1 function, i.e., $u|_K \in (H^1(K))^3$ on each $K \in \mathcal{T}_H$. We then have

$$\delta_i^{-2}\|\boldsymbol{u}\|_{0,\Omega_{i,\delta}}^2 \leqslant C \sum_{j \in I_i} \sum_{K \in \mathcal{T}_{H}} \left[\left(1 + \frac{H_i}{\delta_i}\right) |\boldsymbol{u}|_{1,K}^2 + \frac{1}{\delta_i H_i} \|\boldsymbol{u}\|_{0,K}^2 \right].$$

4.2 Regular decompositions for vector fields

The discrete orthogonal regular decompositions provided in [8], [9] have the following forms:

$$\mathcal{N}\mathcal{D}_{h} = \nabla \mathcal{S}_{h} \oplus \mathcal{N}\mathcal{D}_{h}^{\perp},$$

$$\mathcal{R}\mathcal{T}_{h} = \operatorname{curl} \mathcal{N}\mathcal{D}_{h} \oplus \mathcal{R}\mathcal{T}_{h}^{\perp},$$
(10)

where \mathcal{ND}_h^{\perp} and \mathcal{RT}_h^{\perp} are orthogonal complements. Due to the orthogonality, the stabilities of the decompositions (10) can be anticipated straightforwardly. However, categorizing the orthogonal complements \mathcal{ND}_h^{\perp} and \mathcal{RT}_h^{\perp} poses a significant challenge, hindering the development of effective analytical techniques for the study of overlapping Schwarz methods. In order to overcome this difficulty, the authors of [8], [9] have considered an additional assumption, the convexity of the domain, which enables an embedding into a related space with H¹, already equipped with numerous tools.

Due to a limitation of the orthogonal decomposition, a new approach of regular decompositions was developed in [21]. For each $u_h \in \mathcal{ND}_h$ and $p_h \in \mathcal{RT}_h$, the decompositions are given in the following forms:

$$u_{h} = \nabla \overline{\chi}_{h} + \Pi_{h}^{\mathcal{N}D} \overline{w}_{h} + \widetilde{\overline{u}}_{h},$$

$$p_{h} = \operatorname{curl} \overline{\rho}_{h} + \Pi_{h}^{\mathcal{R}T} \overline{r}_{h} + \widetilde{\overline{p}}_{h},$$
(11)

where $\overline{\chi}_h \in S_h$, $\overline{\boldsymbol{w}}_h \in (S_h)^3$, $\overline{\boldsymbol{u}}_h \in \mathcal{N}D_h$, $\overline{\boldsymbol{\rho}}_h \in \mathcal{N}D_h$, $\overline{\boldsymbol{r}}_h \in (S_h)^3$, $\overline{\boldsymbol{p}}_h \in \mathcal{R}\mathcal{T}_h$, and satisfy some stabilities. Compared to the orthogonal decompositions in (10), the decompositions in (11) are no longer orthogonal. There are also additional oscillatory terms, \tilde{u}_h and \tilde{p}_h . However, (11) provides well-established theories that do not require the assumption of convexity of the domain. As long as the domain is topologically equivalent to a sphere, we can expect the stabilities of the decompositions. We note that the results in (11) have been successfully applied to the theories in [10], [15].

Our next goal is to consider more generally shaped domains, e.g., domains with holes. Note that the decompositions in (11) are based on standard interpolating operators $\Pi_h^{\mathcal{N}\mathcal{D}}$ and $\Pi_h^{\mathcal{R}\mathcal{T}}$. As we have briefly mentioned in Remarks 1 and 2, we need additional regularities in the theories. This may restrict the appropriate topological class of domains. To avoid this restriction, new types of projection operators, which do not require any regularity assumptions, have to be considered. To do so, we first introduce the cochain projections introduced in [25] and extended in [22], [23]. Let

$$\begin{split} \pi_h^{\mathcal{N}D} &: H(\mathbf{curl}; \Omega) \to \mathcal{N}D_h, \\ \pi_h^{\mathcal{RT}} &: H(\mathrm{div}; \Omega) \to \mathcal{RT}_h, \\ \pi_h^0 &: L^2(\Omega) \to P_0(\Omega) \end{split}$$

denote the cochain projection operators constructed in [25] and [22]. We note that the operators satisfy the commuting properties on each element in \mathcal{T}_h

$$\operatorname{curl}\left(\pi_{h}^{\mathcal{N}D}\boldsymbol{u}\right) = \pi_{h}^{\mathcal{R}\mathcal{T}}\left(\operatorname{curl}\boldsymbol{u}\right) \qquad \forall \boldsymbol{u} \in H(\operatorname{curl};\Omega),$$

$$\operatorname{div}\left(\pi_{h}^{\mathcal{R}\mathcal{T}}\boldsymbol{p}\right) = \pi_{h}^{0}\left(\operatorname{div}\boldsymbol{p}\right) \qquad \forall \boldsymbol{p} \in H(\operatorname{div};\Omega)$$
(12)

and the local stability estimates

$$\left\| \pi_{h}^{\mathcal{N}D} \boldsymbol{u} \right\|_{0,K} \leq C \left(\|\boldsymbol{u}\|_{0,\omega_{K}} + h_{K} \|\mathbf{curl} \, \boldsymbol{u}\|_{0,\omega_{K}} \right) \qquad \forall \boldsymbol{u} \in H(\mathbf{curl}; \Omega),$$

$$\left\| \pi_{h}^{\mathcal{R}T} \boldsymbol{p} \right\|_{0,K} \leq C \left(\|\boldsymbol{p}\|_{0,\omega_{K}} + h_{K} \|\mathbf{div} \, \boldsymbol{p}\|_{0,\omega_{K}} \right) \qquad \forall \boldsymbol{p} \in H(\mathbf{div}; \Omega),$$

$$\left\| \pi_{h}^{0} \boldsymbol{z} \right\|_{0,K} \leq C \|\boldsymbol{z}\|_{0,\omega_{K}} \qquad \forall \boldsymbol{z} \in L^{2}(\Omega),$$

$$(13)$$

where $K \in \mathcal{T}_h$, h_K is the diameter of K, and ω_K is the union of the neighboring elements of K. We also remark that the fact that $\boldsymbol{u}_h = \pi_h^{\mathcal{N}D} \boldsymbol{u}_h$ for all $\boldsymbol{u}_h \in \mathcal{N}D_h$ and $\boldsymbol{p}_h = \pi_h^{\mathcal{R}\mathcal{T}} \boldsymbol{p}_h$ for all $\boldsymbol{p}_h \in \mathcal{R}\mathcal{T}_h$, the inverse inequality, (13), and a standard Bramble-Hilbert argument ensure the estimates

$$\left\| \boldsymbol{w}_{h} - \boldsymbol{\pi}_{h}^{\mathcal{N}D} \boldsymbol{w}_{h} \right\|_{0} \leqslant C h \| \nabla \boldsymbol{w}_{h} \|_{0} \tag{14}$$

and

$$\left\| \boldsymbol{w}_h - \boldsymbol{\pi}_h^{\mathcal{R}\mathcal{T}} \boldsymbol{w}_h \right\|_0 \leqslant C h \| \nabla \boldsymbol{w}_h \|_0 \tag{15}$$

for all $\boldsymbol{w}_h \in (S_h)^3$.

We next consider the following regular decomposition in [24, Thm. 10] for edge elements.

Lemma 5 (Hiptmair–Pechstein decomposition for edge elements). For each $u_h \in \mathcal{ND}_h$, there exist a continuous and piecewise linear scalar function $\chi_h \in S_h$, a continuous and piecewise linear vector field $\mathbf{w}_h \in (S_h)^3$, and a remainder $\widetilde{u}_h \in \mathcal{ND}_h$, all depending linearly on u_h , providing the discrete regular decomposition

$$\boldsymbol{u}_h = \nabla \chi_h + \pi_h^{\mathcal{N}D} \boldsymbol{w}_h + \widetilde{\boldsymbol{u}}_h \tag{16}$$

and satisfying the stability estimates

$$\|\nabla \chi_h\|_0 + \|\boldsymbol{w}_h\|_0 + \|\widetilde{\boldsymbol{u}}_h\|_0 \leqslant C\|\boldsymbol{u}_h\|_0, \tag{17}$$

$$\|\nabla \boldsymbol{w}_h\|_0 + \|\widetilde{h}^{-1}\widetilde{\boldsymbol{u}}_h\|_0 \le C(\|\operatorname{curl}\boldsymbol{u}_h\|_0 + \|\boldsymbol{u}_h\|_0),$$
 (18)

where C is a generic constant that depends only on the shape of Ω , but not on the shape-regularity constant of \mathcal{T}_h . Here, h is the piecewise constant function that is equal to h_K on every element $K \in \mathcal{T}_h$.

The regular decomposition in [24, Thm. 13] for face elements is given in the following lemma.

Lemma 6 (Hiptmair–Pechstein decomposition for face elements). For each $p_h \in \mathcal{RT}_h$, there exist a vector field $\rho_h \in \mathcal{ND}_h$, a continuous and piecewise linear vector field $\mathbf{r}_h \in (S_h)^3$, and a remainder $\widetilde{\mathbf{p}}_h \in \mathcal{RT}_h$, all depending linearly on p_h , providing the discrete regular decomposition

$$\boldsymbol{p}_h = \operatorname{curl} \boldsymbol{\rho}_h + \boldsymbol{\pi}_h^{\mathcal{R}\mathcal{T}} \boldsymbol{r}_h + \widetilde{\boldsymbol{p}}_h \tag{19}$$

with the bounds

$$\|\mathbf{curl}\,\rho_h\|_0 + \|\rho_h\|_0 + \|r_h\|_0 + \|\widetilde{p}_h\|_0 \le C\|p_h\|_0,$$
 (20)

$$\|\nabla r_h\|_0 + \|\widetilde{h}^{-1}\widetilde{p}_h\|_0 \le C(\|\operatorname{div} p_h\|_0 + \|p_h\|_0),$$
 (21)

where C is a generic constant that depends only on the shape of Ω , but not on the shape-regularity constant of \mathcal{T}_{h} . Here, h is the piecewise constant function that is equal to h_K on every element $K \in \mathcal{T}_h$.

Remark 3. The Hiptmair-Pechstein decompositions in (16) and (19) are in the same spirit as those in (11), i.e., additional oscillatory components, \tilde{u}_h and \tilde{p}_h , and no orthogonality. Therefore, (16) and (19) are a generalized versions of (11) and good alternatives to (10), since they can provide useful tools for establishing domain decomposition theories, that are more robust to the topology of the domain.

Remark 4. We consider u_h , $u_{1,h}$, and $u_{2,h}$, all in \mathcal{ND}_h , with $u_h = u_{1,h} + u_{2,h}$. Based on Lemma 5, we can construct the decompositions

$$\mathbf{u}_h = \nabla \chi_h + \pi_h^{\mathcal{N}D} \mathbf{w}_h + \widetilde{\mathbf{u}}_h,$$

$$\mathbf{u}_{1,h} = \nabla \chi_{1,h} + \pi_h^{\mathcal{N}D} \mathbf{w}_{1,h} + \widetilde{\mathbf{u}}_{1,h},$$

and

$$\boldsymbol{u}_{2,h} = \nabla \chi_{2,h} + \pi_h^{\mathcal{N}D} \boldsymbol{w}_{2,h} + \widetilde{\boldsymbol{u}}_{2,h}.$$

Then, $\chi_h = \chi_{1,h} + \chi_{2,h}$, $\boldsymbol{w}_h = \boldsymbol{w}_{1,h} + \boldsymbol{w}_{2,h}$ and $\widetilde{\boldsymbol{u}}_h = \widetilde{\boldsymbol{u}}_{1,h} + \widetilde{\boldsymbol{u}}_{2,h}$. We also have a similar linearity for face elements associated with Lemma 6.

4.3 Schwarz framework

In this subsection, we summarize the abstract Schwarz framework, a key ingredient for analyzing domain decomposition methods. For more detail, see [19, Ch. 2].

Lemma 7. If for all $\mathbf{u}_h \in \mathcal{N}\mathcal{D}_h$ there is a representation, $\mathbf{u}_h = \sum_{i=0}^N \mathbf{u}_i$, where $\mathbf{u}_0 \in \mathcal{N}\mathcal{D}_H$ and $\mathbf{u}_i \in \mathcal{N}\mathcal{D}_h^{(i)}$ for $i = 1, 2, \dots, N$, such that

$$\sum_{i=0}^{N} a_c(\boldsymbol{u}_i, \boldsymbol{u}_i) \leqslant C_c^2 a_c(\boldsymbol{u}_h, \boldsymbol{u}_h),$$

then the smallest eigenvalue of the preconditioned linear operator defined in (9) is bounded from below by C_c^{-2} .

Lemma 8. If for all $p_h \in \mathcal{RT}_h$ there is a representation, $p_h = \sum_{i=0}^N p_i$, where $p_0 \in \mathcal{RT}_H$ and $p_i \in \mathcal{RT}_h^{(i)}$ for $i = 1, 2, \dots, N$, such that

$$\sum_{i=0}^{N} a_d(\boldsymbol{p}_i, \boldsymbol{p}_i) \leqslant C_d^2 a_d(\boldsymbol{p}_h, \boldsymbol{p}_h),$$

then the smallest eigenvalue of the preconditioned linear operator defined in (9) is bounded from below by C_d^{-2} .

Lemma 9. The largest eigenvalue of the operator introduced in (9) is bounded from above by $N_0 + 1$, where N_0 is defined in Assumption 2.

4.4 Condition number estimate for H(curl)

For elliptic equations, which have a global dependence of the solution due to the Green's function representation, the solution is generally nonzero throughout the entire domain, even if the forcing term or the boundary value is nonzero only within a small subregion. Numerical algorithms for solving elliptic problems have to take this characteristic into account. In overlapping Schwarz methods, each iteration transfers information only between

neighboring subdomains. Hence, several iterations may be required for the local change to be effective across the entire domain without the incorporation of a global component, also known as a coarse component. We also remark that, based on numerical experiments in [27], the constant C_c^2 in Lemma 7, which plays an important role in the performance of the preconditioner, is $O(1/(\delta H))$, where H is the diameter of the subdomain and δ is the size of the overlap between subdomains, excluding the coarse component u_0 . We therefore need a suitable coarse component to find a good bound in Lemma 7.

Based on Lemma 5, for any $\boldsymbol{u}_h \in \mathcal{ND}_h$, we can find $\boldsymbol{\chi}_h$, \boldsymbol{w}_h , and $\widetilde{\boldsymbol{u}}_h$, which satisfy (17) and (18). We then consider

$$\mathbf{u}_0 := \nabla \chi_0 + \mathbf{w}_0,
\mathbf{u}_i := \nabla \chi_i + \mathbf{w}_i + \widetilde{\mathbf{u}}_i, \quad i = 1, 2, \dots, N,$$
(22)

where

$$\chi_{0} = \widetilde{\Pi}_{H}^{S} \chi_{h},
\boldsymbol{w}_{0} = Q_{H}^{ND} \boldsymbol{w}_{h},
\chi_{i} = \Pi_{h}^{S} (\theta_{i} (\chi_{h} - \chi_{0})),
\boldsymbol{w}_{i} = \Pi_{h}^{ND} (\theta_{i} (\pi_{h}^{ND} \boldsymbol{w}_{h} - \boldsymbol{w}_{0})),
\widetilde{\boldsymbol{u}}_{i} = \Pi_{h}^{ND} (\theta_{i} \widetilde{\boldsymbol{u}}_{h}).$$
(23)

Here, the interpolation operators $\widetilde{\Pi}_{H}^{S}$, Π_{h}^{S} , and $\Pi_{h}^{\mathcal{N}D}$ are defined in Section 2 and the set $\{\theta_{i}\}$, the L^{2} -projection operator $Q_{H}^{\mathcal{N}D}$, and the cochain projection $\pi_{h}^{\mathcal{N}D}$ are mentioned in Section 3, 4.1, and 4.2, respectively. From (22) and (23), we can easily check $\mathbf{u}_{0} \in \mathcal{N}D_{H}$, $\mathbf{u}_{i} \in \mathcal{N}D_{h}^{(i)}$, and $\mathbf{u}_{h} = \sum_{i=0}^{N} \mathbf{u}_{i}$. We separately estimate the coarse component \mathbf{u}_{0} and the local components, i.e., \mathbf{u}_{i} , $i=1,\ldots,N$.

We first consider the coarse component. The next lemma shows the stability of u_0 .

Lemma 10. Assume that the constant η_c in (2) is less than or equal to one. Then, we have the following estimate for the coarse component in (22):

$$a_c(\mathbf{u}_0, \mathbf{u}_0) \leqslant Ca_c(\mathbf{u}_h, \mathbf{u}_h), \tag{24}$$

where the constant C does not depend on N, h, H_i , δ_i , and η_c .

Proof. We note that $\mathbf{u}_0 = \nabla \chi_0 + \mathbf{w}_0$. We estimate each term separately.

– Term χ_0 :

From the property of Scott–Zhang interpolation, i.e., the operator $\widetilde{\Pi}_h^S$ is stable with respect to the H^1 -norm, and (17), we have

$$a_{c}(\nabla \chi_{0}, \nabla \chi_{0}) = \|\nabla \chi_{0}\|_{0}^{2} \leqslant C \|\nabla \chi_{h}\|_{0}^{2} \leqslant C \|\boldsymbol{u}_{h}\|_{0}^{2}. \tag{25}$$

– Term \boldsymbol{w}_0 :

By using the definition of $Q_H^{\mathcal{N}D}$ and (17), we obtain

$$\|\boldsymbol{w}_0\|_0^2 = \|Q_H^{\mathcal{N}D}\boldsymbol{w}_h\|_0^2 \le \|\boldsymbol{w}_h\|_0^2 \le C\|\boldsymbol{u}_h\|_0^2.$$
 (26)

Due to Lemma 1 and (18), we have

$$\eta_{c} \|\mathbf{curl} \, \boldsymbol{w}_{0}\|_{0}^{2} = \eta_{c} \|\mathbf{curl} \left(Q_{H}^{ND} \boldsymbol{w}_{h}\right)\|_{0}^{2} \leqslant C \eta_{c} \|\nabla \boldsymbol{w}_{h}\|_{0}^{2}
\leqslant C \left(\eta_{c} \|\boldsymbol{u}_{h}\|_{0}^{2} + \eta_{c} \|\mathbf{curl} \, \boldsymbol{u}_{h}\|_{0}^{2}\right) \leqslant C a_{c}(\boldsymbol{u}_{h}, \boldsymbol{u}_{h}).$$
(27)

Hence, by combining (25), (26), and (27) and using Cauchy–Schwarz inequality, the estimate (24) holds.

We next consider an estimate for local components. Since the proof of the lemma is overlong, we estimate each term in (22) individually using propositions and put them together later.

Proposition 1. Consider χ_i defined in (23) and assume that $\eta_c \leq 1$. Then, we have

$$\sum_{i=1}^{N} a_c(\nabla \chi_i, \nabla \chi_i) \leq C\left(\max_{1 \leq i \leq N} \left(1 + \frac{H_i}{\delta_i}\right)\right) a_c(\boldsymbol{u}_h, \boldsymbol{u}_h),$$

where the constant C is independent from N, h, H_i , δ_i , and η_c .

Proof. We have the following estimate from [19, Lem. 3.12] and (17):

$$\begin{split} \sum_{i=1}^{N} a_{c} \left(\nabla \chi_{i}, \nabla \chi_{i} \right) & \leq C \left(\max_{1 \leq i \leq N} \left(1 + \frac{H_{i}}{\delta_{i}} \right) \right) \left\| \nabla \chi_{h} \right\|_{0}^{2} \\ & \leq C \left(\max_{1 \leq i \leq N} \left(1 + \frac{H_{i}}{\delta_{i}} \right) \right) \left\| \boldsymbol{u}_{h} \right\|_{0}^{2} \\ & \leq C \left(\max_{1 \leq i \leq N} \left(1 + \frac{H_{i}}{\delta_{i}} \right) \right) a_{c} \left(\boldsymbol{u}_{h}, \boldsymbol{u}_{h} \right). \end{split}$$

Proposition 2. Consider w_i defined in (23) and assume that $\eta_c \leq 1$. Then, we have

$$\sum_{i=1}^{N} a_{c}(\boldsymbol{w}_{i}, \boldsymbol{w}_{i}) \leq C \left(\max_{1 \leq i \leq N} \left(1 + \frac{H_{i}}{\delta_{i}} \right) \right) a_{c}(\boldsymbol{u}_{h}, \boldsymbol{u}_{h}),$$

where the constant C is independent from N, h, H_i , δ_i , and η_c .

Proof. By using Lemma 3, the properties of θ_i in (8), the triangle inequality, (13), the inverse estimate, the finite covering property in Assumption 2, (26), and (17), we obtain

$$\sum_{i=1}^{N} \|\boldsymbol{w}_{i}\|_{0,\Omega_{i}^{\prime}}^{2} \leq C \sum_{i=1}^{N} \|\theta_{i} (\pi_{h}^{\mathcal{N}D} \boldsymbol{w}_{h} - \boldsymbol{w}_{0})\|_{0,\Omega_{i}^{\prime}}^{2} \leq C (\|\boldsymbol{w}_{h}\|_{0}^{2} + \|\boldsymbol{w}_{0}\|_{0}^{2})$$

$$\leq C \|\boldsymbol{w}_{h}\|_{0}^{2} \leq C \|\boldsymbol{u}_{h}\|_{0}^{2}. \tag{28}$$

Let ${m v}_1=\pi_h^{\mathcal ND}{m w}_h-{m w}_h, {m v}_2={m w}_h-{m w}_0={m w}_h-Q_H^{\mathcal ND}{m w}_h$, and ${m v}={m v}_1+{m v}_2$. Due to Lemma 3, the construction of θ_i , Assumption 2, and the triangle inequality, we have

$$\sum_{i=1}^{N} \eta_{c} \|\mathbf{curl} \, \boldsymbol{w}_{i}\|_{0,\Omega_{i}^{\prime}}^{2} \leq C \eta_{c} \|\mathbf{curl} \, \boldsymbol{v}\|_{0}^{2} + C \eta_{c} \sum_{i=1}^{N} \delta_{i}^{-2} \|\boldsymbol{v}\|_{0,\Omega_{i,\delta}}^{2}$$

$$\leq C \eta_{c} \|\mathbf{curl} \, \boldsymbol{v}\|_{0}^{2} + C \eta_{c} \sum_{i=1}^{N} \delta_{i}^{-2} \|\boldsymbol{v}_{1}\|_{0,\Omega_{i,\delta}}^{2} + C \eta_{c} \sum_{i=1}^{N} \delta_{i}^{-2} \|\boldsymbol{v}_{2}\|_{0,\Omega_{i,\delta}}^{2}$$

$$:= E_{1} + E_{2} + E_{3}. \tag{29}$$

We first consider E_1 . By using the triangle inequality, Lemma 1, (12), (13), and (18), we obtain

$$E_{1} = C\eta_{c} \|\mathbf{curl} \, \boldsymbol{v}\|_{0}^{2} \leqslant C\eta_{c} \|\mathbf{curl} \left(\pi_{h}^{\mathcal{N}D} \boldsymbol{w}_{h}\right)\|_{0}^{2} + C\eta_{c} \|\mathbf{curl} \left(Q_{H}^{\mathcal{N}D} \boldsymbol{w}_{h}\right)\|_{0}^{2}$$

$$\leqslant C\eta_{c} \|\pi_{h}^{\mathcal{R}\mathcal{T}} \left(\mathbf{curl} \, \boldsymbol{w}_{h}\right)\|_{0}^{2} + C\eta_{c} \|\nabla \boldsymbol{w}_{h}\|_{0}^{2} \leqslant C\eta_{c} \|\mathbf{curl} \, \boldsymbol{w}_{h}\|_{0}^{2} + C\eta_{c} \|\nabla \boldsymbol{w}_{h}\|_{0}^{2} \leqslant C\eta_{c} \|\nabla \boldsymbol{w}_{h}\|_{0}^{2}$$

$$\leqslant C\left(\eta_{c} \|\boldsymbol{u}_{h}\|_{0}^{2} + \eta_{c} \|\mathbf{curl} \, \boldsymbol{u}_{h}\|_{0}^{2}\right) \leqslant Ca_{c}(\boldsymbol{u}_{h}, \boldsymbol{u}_{h}). \tag{30}$$

Regarding E_2 , the following estimate holds from the error estimate (14), the finite covering property in Assumption 2, and (18):

$$E_{2} = C\eta_{c} \sum_{i=1}^{N} \delta_{i}^{-2} \|\boldsymbol{v}_{1}\|_{0,\Omega_{i,\delta}}^{2} \leq C\eta_{c} \sum_{i=1}^{N} h^{-2} \|\boldsymbol{\pi}_{h}^{\mathcal{N}D} \boldsymbol{w}_{h} - \boldsymbol{w}_{h} \|_{0,\Omega_{i}'}^{2}$$

$$\leq C\eta_{c} \|\nabla \boldsymbol{w}_{h}\|_{0}^{2} \leq C \left(\eta_{c} \|\boldsymbol{u}_{h}\|_{0}^{2} + \eta_{c} \|\mathbf{curl} \, \boldsymbol{u}_{h}\|_{0}^{2}\right)$$

$$\leq Ca_{c}(\boldsymbol{u}_{h}, \boldsymbol{u}_{h}). \tag{31}$$

We finally estimate E_3 . Lemma 4 implies

$$E_{3} = C\eta_{c} \sum_{i=1}^{N} \delta_{i}^{-2} \|\boldsymbol{v}_{2}\|_{0,\Omega_{i,\delta}}^{2}$$

$$\leq C\eta_{c} \sum_{i=1}^{N} \sum_{j \in I_{i}} \sum_{K \in \mathcal{T}_{H}, K \in \overline{\Omega}_{j}} \left(1 + \frac{H_{i}}{\delta_{i}}\right) |\boldsymbol{v}_{2}|_{1,K}^{2} + C\eta_{c} \sum_{i=1}^{N} \sum_{j \in I_{i}} \sum_{K \in \mathcal{T}_{H}, K \in \overline{\Omega}_{j}} \frac{1}{\delta_{i} H_{i}} \|\boldsymbol{v}_{2}\|_{0,K}^{2}$$

$$:= E_{3.1} + E_{3.2}. \tag{32}$$

We have the following estimate from the triangle inequality, the inverse estimate, and Lemma 2:

$$|\mathbf{v}_{2}|_{1,K} = |\mathbf{w}_{h} - Q_{H}^{\mathcal{N}D}\mathbf{w}_{h}|_{1,K} \leq |\mathbf{w}_{h}|_{1,K} + |Q_{H}^{\mathcal{N}D}\mathbf{w}_{h}|_{1,K}$$

$$= |\mathbf{w}_{h}|_{1,K} + |Q_{H}^{\mathcal{N}D}\mathbf{w}_{h} - Q_{H,K}^{0}\mathbf{w}_{h}|_{1,K}$$

$$\leq |\mathbf{w}_{h}|_{1,K} + CH^{-1} \|Q_{H}^{\mathcal{N}D}\mathbf{w}_{h} - Q_{H,K}^{0}\mathbf{w}_{h}\|_{0,K}$$

$$\leq |\mathbf{w}_{h}|_{1,K} + CH^{-1} \|Q_{H}^{\mathcal{N}D}\mathbf{w}_{h} - \mathbf{w}_{h}\|_{0,K} + CH^{-1} \|\mathbf{w}_{h} - Q_{H,K}^{0}\mathbf{w}_{h}\|_{0,K}$$

$$\leq C|\mathbf{w}_{h}|_{1,K} + CH^{-1} \|Q_{H}^{\mathcal{N}D}\mathbf{w}_{h} - \mathbf{w}_{h}\|_{0,K}.$$
(33)

Let $\Xi = \max_{1 \le i \le n} (H_i / \delta_i)$. Then, by using (33), Lemma 1 and (18), we have

$$E_{3,1} = C\eta_{c} \sum_{i=1}^{N} \sum_{j \in I_{i}} \sum_{K \in \mathcal{T}_{H}, \atop K \subset \overline{\Omega}_{j}} \left(1 + \frac{H_{i}}{\delta_{i}}\right) |\boldsymbol{v}_{2}|_{1,K}^{2} \leqslant C\eta_{c}(1 + \Xi) \sum_{i=1}^{N} \sum_{j \in I_{i}} \sum_{K \in \mathcal{T}_{H}, \atop K \subset \overline{\Omega}_{j}} |\boldsymbol{v}_{2}|_{1,K}^{2}$$

$$\leqslant \eta_{c}(1 + \Xi) \left(C \sum_{i=1}^{N} \sum_{j \in I_{i}} \sum_{K \in \mathcal{T}_{H}, \atop K \subset \overline{\Omega}_{j}} |\boldsymbol{w}_{h}|_{1,K}^{2} + CH^{-2} \sum_{i=1}^{N} \sum_{j \in I_{i}} \sum_{K \in \mathcal{T}_{H}, \atop K \subset \overline{\Omega}_{j}} |\boldsymbol{Q}_{H}^{ND} \boldsymbol{w}_{h} - \boldsymbol{w}_{h}|_{0,K}^{2} \right)$$

$$\leqslant \eta_{c}(1 + \Xi) \left(C ||\nabla \boldsymbol{w}_{h}||_{0}^{2} + CH^{-2} ||\boldsymbol{Q}_{H}^{ND} \boldsymbol{w}_{h} - \boldsymbol{w}_{h}||_{0}^{2} \right) \leqslant C\eta_{c}(1 + \Xi) ||\nabla \boldsymbol{w}_{h}||_{0}^{2}$$

$$\leqslant C(1 + \Xi) \left(\eta_{c} ||\boldsymbol{u}_{h}||_{0}^{2} + \eta_{c} ||\operatorname{\mathbf{curl}} \boldsymbol{u}_{h}||_{0}^{2} \right) \leqslant C(1 + \Xi) a_{c}(\boldsymbol{u}_{h}, \boldsymbol{u}_{h}). \tag{34}$$

Moreover, from Assumption 3, Lemma 1, and (18), we obtain

$$E_{3,2} = C\eta_c \sum_{i=1}^{N} \sum_{j \in I_i} \sum_{K \in \mathcal{T}_H, \atop K \subset \overline{\Omega}_j} \frac{1}{\delta_i H_i} \| \boldsymbol{v}_2 \|_{0,K}^2 \leqslant C\eta_c H^{-2} \sum_{i=1}^{N} \sum_{j \in I_i} \sum_{K \in \mathcal{T}_H, \atop K \subset \overline{\Omega}_j} \frac{H_i}{\delta_i} \| Q_H^{\mathcal{N}D} \boldsymbol{w}_h - \boldsymbol{w}_h \|_{0,K}^2$$

$$\leq C\eta_{c}\Xi H^{-2} \|Q_{H}^{\mathcal{N}D}\boldsymbol{w}_{h} - \boldsymbol{w}_{h}\|_{0}^{2} \leq C\eta_{c}\Xi \|\nabla \boldsymbol{w}_{h}\|_{0}^{2}
\leq C\Xi (\eta_{c}\|\boldsymbol{u}_{h}\|_{0}^{2} + \eta_{c}\|\operatorname{curl}\boldsymbol{u}_{h}\|_{0}^{2}) \leq C\Xi a_{c}(\boldsymbol{u}_{h}, \boldsymbol{u}_{h}).$$
(35)

Thus, by using (29), (30), (31), (32), (34), and (35), the following estimate holds:

$$\sum_{i=1}^{N} \eta_c \|\mathbf{curl}\,\boldsymbol{w}_i\|_{0,\Omega_i'}^2 \leqslant C \max_{1 \leqslant i \leqslant N} \left(1 + \frac{H_i}{\delta_i}\right) a_c(\boldsymbol{u}_h, \boldsymbol{u}_h). \tag{36}$$

Combining (28) and (36), we have

$$\sum_{i=1}^{N} a_{c}(\boldsymbol{w}_{i}, \boldsymbol{w}_{i}) \leqslant C\left(\max_{1 \leqslant i \leqslant N} \left(1 + \frac{H_{i}}{\delta_{i}}\right)\right) a_{c}(\boldsymbol{u}_{h}, \boldsymbol{u}_{h}).$$

Proposition 3. Consider \widetilde{u}_i defined in (23) and assume that $\eta_c \leqslant$ 1. Then, we have

$$\sum_{i=1}^{N} a_{c}(\widetilde{\boldsymbol{u}}_{i}, \widetilde{\boldsymbol{u}}_{i}) \leqslant a_{c}(\boldsymbol{u}_{h}, \boldsymbol{u}_{h}),$$

where the constant C is independent from N, h, H_i , δ_i , and η_c .

Proof. From Lemma 3, (8), Assumption 2, the inverse inequality, (17), and (18), we have

$$\sum_{i=1}^{N} \|\widetilde{\boldsymbol{u}}_{i}\|_{0,\Omega_{i}'}^{2} \leq C \sum_{i=1}^{N} \|\theta_{i}\widetilde{\boldsymbol{u}}_{h}\|_{0,\Omega_{i}'}^{2} \leq C \|\widetilde{\boldsymbol{u}}_{h}\|_{0}^{2} \leq C \|\boldsymbol{u}_{h}\|_{0}^{2}$$
(37)

and

$$\sum_{i=1}^{N} \eta_{c} \|\mathbf{curl}\,\widetilde{\boldsymbol{u}}_{i}\|_{0,\Omega_{i}^{\prime}}^{2} \leq C \eta_{c} \sum_{i=1}^{N} \delta_{i}^{-2} \|\widetilde{\boldsymbol{u}}_{h}\|_{0,\Omega_{i}^{\prime}}^{2} + C \eta_{c} \|\mathbf{curl}\,\widetilde{\boldsymbol{u}}_{h}\|_{0}^{2} \leq C \eta_{c} h^{-2} \|\widetilde{\boldsymbol{u}}_{h}\|_{0}^{2}$$

$$\leq C \left(\eta_{c} \|\boldsymbol{u}_{h}\|_{0}^{2} + \eta_{c} \|\mathbf{curl}\,\boldsymbol{u}_{h}\|_{0}^{2}\right) \leq C a_{c}(\boldsymbol{u}_{h}, \boldsymbol{u}_{h}). \tag{38}$$

We therefore have

$$\sum_{i=1}^{N} a_{c}(\widetilde{\boldsymbol{u}}_{i}, \widetilde{\boldsymbol{u}}_{i}) \leqslant Ca_{c}(\boldsymbol{u}_{h}, \boldsymbol{u}_{h}).$$

Lemma 11. Assume that the constant η_c in (2) is less than or equal to one. Then, we have the following estimate for the local components in (22):

$$\sum_{i=1}^{N} a_{c}(\boldsymbol{u}_{i}, \boldsymbol{u}_{i}) \leq C \left(\max_{1 \leq i \leq N} \left(1 + \frac{H_{i}}{\delta_{i}} \right) \right) a_{c}(\boldsymbol{u}_{h}, \boldsymbol{u}_{h}), \tag{39}$$

where the constant C does not depend on N, h, H_i , δ_i , and η_c .

Proof. Based on Propositions 1, 2, and 3, we have (39).

We finally have an estimate of the condition number for our $H(\mathbf{curl})$ model problem.

Theorem 1. Let $\eta_c \leq 1$. We then have the following estimate:

$$\varkappa \left(M_c^{-1} A_c \right) \leqslant C \max_{1 \leqslant i \leqslant N} \left(1 + \frac{H_i}{\delta_i} \right), \tag{40}$$

where the constant C does not depend on the mesh sizes, H_i , δ_i , η_c , and the number of subdomains but may depend on N_0 .

Proof. We have (40) from Lemmas 7, 9, 10, and 11.

Corollary 1. If the first Betti number of the domain Ω , i.e., the number of circular holes, vanishes, we have (40) in Theorem 1 without the assumption $\eta_c \leq 1$.

Proof . If the first Betti number of the domain Ω vanishes, we have a more favorable bound in (18), i.e., the right hand side can be replaced by the curl term only. Thus, we can have (40) in Theorem 1 without the assumption $\eta_c \leq 1$. For more detail, see [22, Sect. 5.1].

4.5 Condition number estimate for H(div)

Like the $H(\mathbf{curl})$ case, we consider the following decomposition for any $\mathbf{p}_h \in \mathcal{RT}_h$ based on Lemma 6:

$$\begin{aligned}
\mathbf{p}_0 &:= \operatorname{curl} \boldsymbol{\sigma}_0 + \mathbf{r}_0, \\
\mathbf{p}_i &:= \operatorname{curl} \left(\boldsymbol{\sigma}_i + \widetilde{\boldsymbol{\rho}}_i \right) + \mathbf{r}_i + \widetilde{\mathbf{p}}_i, \quad i = 1, 2, \dots, N,
\end{aligned} \tag{41}$$

where

$$\sigma_{0} = Q_{H}^{\mathcal{N}D}\sigma_{h},$$

$$r_{0} = Q_{H}^{\mathcal{R}T}\mathbf{r}_{h},$$

$$\sigma_{i} = \Pi_{h}^{\mathcal{N}D}\left(\theta_{i}\left(\pi_{h}^{\mathcal{N}D}\sigma_{h} - \sigma_{0}\right)\right),$$

$$\tilde{\rho}_{i} = \Pi_{h}^{\mathcal{N}D}\left(\theta_{i}\tilde{\rho}_{h}\right),$$

$$r_{i} = \Pi_{h}^{\mathcal{R}T}\left(\theta_{i}\left(\pi_{h}^{\mathcal{R}T}\mathbf{r}_{h} - \mathbf{r}_{0}\right)\right),$$

$$\tilde{p}_{i} = \Pi_{h}^{\mathcal{R}T}\left(\theta_{i}\tilde{\rho}_{h}\right).$$
(42)

Here, $\rho_h = \nabla \mu_h + \Pi_h^{\mathcal{N}D} \sigma_h + \widetilde{\rho}_h$ is given based on Lemma 5. We note that the operators $\Pi_h^{\mathcal{N}D}$ and $\Pi_h^{\mathcal{R}\mathcal{T}}$ are introduced in Section 2. We also remark that the partition of unity set $\{\theta_i\}$ is constructed in Section 3 and the L^2 -projection operators are defined in Section 4.1. In addition, the cochain projections $\pi_h^{\mathcal{N}D}$ and $\pi_h^{\mathcal{R}\mathcal{T}}$ are introduced in Section 4.2. Obviously, we have $\boldsymbol{p}_0 \in \mathcal{R}\mathcal{T}_H$, $\boldsymbol{p}_i \in \mathcal{R}\mathcal{T}_h^{(i)}$, and $\boldsymbol{p}_h = \sum_{i=0}^N \boldsymbol{p}_i$. Similarly, we consider estimates for the coarse and the local components.

We first consider the stability of p_0 in (41). We recall that we have the constant η_d in the bilinear form (4).

Lemma 12. Assume that the constant η_d in (4) is less than or equal to one. Then, we have the following estimate for the coarse component \mathbf{p}_0 in (41):

$$a_d(\mathbf{p}_0, \mathbf{p}_0) \leqslant Ca_d(\mathbf{p}_h, \mathbf{p}_h), \tag{43}$$

where the constant C does not depend on N, h, H_i , δ_i , and η_d .

Proof. Based on the decomposition $p_0 = \operatorname{curl} \sigma_0 + r_0$, we consider each term one by one.

– Term σ_0 :

With a similar argument to (27) in Lemma 10, (18), and (20), we have

$$a_d(\operatorname{curl}\boldsymbol{\sigma}_0, \operatorname{curl}\boldsymbol{\sigma}_0) = \|\operatorname{curl}\boldsymbol{\sigma}_0\|_0^2 \leqslant C\|\boldsymbol{p}_h\|_0^2. \tag{44}$$

- Term r_0 :

From the projection property and (20), we obtain

$$\|\mathbf{r}_0\|_0^2 = \|Q_H^{\mathcal{R}\mathcal{T}}\mathbf{r}_h\|_0^2 \le \|\mathbf{r}_h\|_0^2 \le C\|\mathbf{p}_h\|_0^2.$$
 (45)

By using Lemma 1 and (21), the following estimate holds:

$$\eta_{d} \|\operatorname{div} \boldsymbol{r}_{0}\|_{0}^{2} = \eta_{d} \|\operatorname{div} \left(Q_{H}^{\mathcal{R}\mathcal{T}} \boldsymbol{r}_{h}\right)\|_{0}^{2} \leqslant C \eta_{d} \|\nabla \boldsymbol{r}_{h}\|_{0}^{2}
\leqslant C \left(\eta_{d} \|\operatorname{div} \boldsymbol{p}_{h}\|_{0}^{2} + \eta_{d} \|\boldsymbol{p}_{h}\|_{0}^{2}\right) \leqslant C a_{d}(\boldsymbol{p}_{h}, \boldsymbol{p}_{h}).$$
(46)

We therefore have (43) from (44), (45), and (46).

We next consider three propositions to estimate each term associated with the local components in (41) separately.

Proposition 4. Assume that $\eta_d \leq 1$. Let $\rho_i = \sigma_i + \widetilde{\rho}_i$, where the terms σ_i and $\widetilde{\rho}_i$ introduced in (42). We then have

$$\sum_{i=1}^N a_d \big(\mathbf{curl} \, \boldsymbol{\rho}_i, \mathbf{curl} \, \boldsymbol{\rho}_i \big) \leqslant C \max_{1 \leqslant i \leqslant N} \bigg(1 + \frac{H_i}{\delta_i} \bigg) a_d \big(\boldsymbol{p}_h, \boldsymbol{p}_h \big),$$

where the constant C is independent from N, h, H_i , δ_i , and η_d .

Proof. We can use the same methods in Propositions 2 and 3 and (20). We then have

$$\begin{split} \sum_{i=1}^{N} a_d \big(\mathbf{curl} \, \boldsymbol{\rho}_i, \mathbf{curl} \, \boldsymbol{\rho}_i \big) &= \sum_{i=1}^{N} \| \mathbf{curl} \, \boldsymbol{\rho}_i \|_{0, \Omega_i'}^2 \leqslant C \max_{1 \leqslant i \leqslant N} \bigg(1 + \frac{H_i}{\delta_i} \bigg) \| \boldsymbol{p}_h \|_0^2 \\ &\leqslant C \max_{1 \leqslant i \leqslant N} \bigg(1 + \frac{H_i}{\delta_i} \bigg) a_d \big(\boldsymbol{p}_h, \boldsymbol{p}_h \big). \end{split}$$

Proposition 5. Assume that $\eta_d \le 1$. Then, the term r_i introduced in (42) has the following estimate:

$$\sum_{i=1}^{N} a_d(\boldsymbol{r}_i, \boldsymbol{r}_i) \leqslant C \max_{1 \leqslant i \leqslant N} \left(1 + \frac{H_i}{\delta_i}\right) a_d(\boldsymbol{p}_h, \boldsymbol{p}_h),$$

where the constant C is independent from N, h, H_i , δ_i , and η_d .

Proof. With the same process with (28), we obtain

$$\sum_{i=1}^{N} \| \boldsymbol{r}_{i} \|_{0,\Omega_{i}^{\prime}}^{2} \leq C \| \boldsymbol{r}_{h} \|_{0}^{2} \leq C \| \boldsymbol{p}_{h} \|_{0}^{2}. \tag{47}$$

Let $q=q_1+q_2$ with $q_1=\pi_h^{\mathcal{RT}} r_h-r_h$ and $q_2=r_h-r_0=r_h-Q_H^{\mathcal{RT}} r_h$. By using a similar argument to (29), we have

$$\sum_{i=1}^{N} \eta_{d} \|\operatorname{div} \mathbf{r}_{i}\|_{0,\Omega_{i}^{\prime}}^{2} \leq C \eta_{d} \|\operatorname{div} \mathbf{q}\|_{0}^{2} + C \eta_{d} \sum_{i=1}^{N} \delta_{i}^{-2} \|\mathbf{q}_{1}\|_{0,\Omega_{i,\delta}}^{2} + C \eta_{d} \sum_{i=1}^{N} \delta_{i}^{-2} \|\mathbf{q}_{2}\|_{0,\Omega_{i,\delta}}^{2}$$

$$:= F_{1} + F_{2} + F_{3}. \tag{48}$$

Regarding F_1 , we obtain the following estimate in a similar way to (30):

$$F_{1} = C\eta_{d} \|\operatorname{div} \boldsymbol{q}\|_{0}^{2} \leqslant C\eta_{d} \|\operatorname{div} \left(\pi_{h}^{\mathcal{R}^{\mathcal{T}}} \boldsymbol{r}_{h}\right)\|_{0}^{2} + C\eta_{d} \|\operatorname{div} \left(Q_{H}^{\mathcal{R}^{\mathcal{T}}} \boldsymbol{r}_{h}\right)\|_{0}^{2}$$

$$\leqslant C\eta_{d} \|\pi_{h}^{0} (\operatorname{div} \boldsymbol{r}_{h})\|_{0}^{2} + C\eta_{d} \|\nabla \boldsymbol{r}_{h}\|_{0}^{2} \leqslant C\eta_{d} \|\operatorname{div} \boldsymbol{r}_{h}\|_{0}^{2} + C\eta_{d} \|\nabla \boldsymbol{r}_{h}\|_{0}^{2}$$

$$\leqslant C\eta_{d} \|\nabla \boldsymbol{r}_{h}\|_{0}^{2} \leqslant C\left(\eta_{d} \|\operatorname{div} \boldsymbol{p}_{h}\|_{0}^{2} + \eta_{d} \|\boldsymbol{p}_{h}\|_{0}^{2}\right)$$

$$\leqslant Ca_{d}(\boldsymbol{p}_{h}, \boldsymbol{p}_{h}). \tag{49}$$

We next estimate F_2 using the similar arguments in (32). The following bound can be found using (15), the finite covering property in Assumption 2, and (21):

$$F_{2} = C\eta_{d} \sum_{i=1}^{N} \delta_{i}^{-2} \|\boldsymbol{q}_{1}\|_{0,\Omega_{i,\delta}} \leq C\eta_{d} \sum_{i=1}^{N} h^{-2} \|\boldsymbol{\pi}_{h}^{\mathcal{R}\mathcal{T}} \boldsymbol{r}_{h} - \boldsymbol{r}_{h}\|_{0,\Omega'_{i}}^{2}$$

$$\leq C\eta_{d} \|\nabla \boldsymbol{r}_{h}\|_{0}^{2} \leq C \left(\eta_{d} \|\operatorname{div} \boldsymbol{p}_{h}\|_{0}^{2} + \eta_{d} \|\boldsymbol{p}_{h}\|_{0}^{2}\right)$$

$$\leq Ca_{d}(\boldsymbol{p}_{h}, \boldsymbol{p}_{h}). \tag{50}$$

Finally, we consider F_3 . Like (32), from Lemma 4, we have

$$F_{3} = C\eta_{d} \sum_{i=1}^{N} \delta_{i}^{-2} \|\mathbf{q}_{2}\|_{0,\Omega_{i,\delta}}^{2}$$

$$\leq C\eta_{d} \sum_{i=1}^{N} \sum_{j \in I_{i}} \sum_{K \in \mathcal{T}_{H}, \\ K \subset \overline{\Omega}_{j}} \left(1 + \frac{H_{i}}{\delta_{i}}\right) |\mathbf{q}_{2}|_{1,K}^{2} + C\eta_{d} \sum_{i=1}^{N} \sum_{j \in I_{i}} \sum_{K \in \mathcal{T}_{H}, \\ K \subset \overline{\Omega}_{j}} \frac{1}{\delta_{i} H_{i}} \|\mathbf{q}_{2}\|_{0,K}^{2}$$

$$:= F_{3,1} + F_{3,2}. \tag{51}$$

In the same way as (33), we obtain

$$|q_2|_{1,K} \le C|r_h|_{1,K} + CH^{-1} \|Q_H^{\mathcal{R}\mathcal{T}}r_h - r_h\|_{0,K}.$$
 (52)

Hence, in a similar way to (34), we have

$$F_{3,1} = C\eta_{d} \sum_{i=1}^{N} \sum_{j \in I_{i}} \sum_{K \in \mathcal{T}_{H}, \\ K \subset \Omega_{j}} \left(1 + \frac{H_{i}}{\delta_{i}} \right) |\boldsymbol{q}_{2}|_{1,K}^{2} \leq C\eta_{d}(1 + \Xi) \sum_{i=1}^{N} \sum_{j \in I_{i}} \sum_{K \in \mathcal{T}_{H}, \\ K \subset \Omega_{j}} |\boldsymbol{q}_{2}|_{1,K}^{2}$$

$$\leq \eta_{d}(1 + \Xi) \left(C \|\nabla \boldsymbol{r}_{h}\|_{0}^{2} + CH^{-2} \|\boldsymbol{Q}_{H}^{\mathcal{R}\mathcal{T}} \boldsymbol{r}_{h} - \boldsymbol{r}_{h}\|_{0}^{2} \right) \leq C\eta_{d}(1 + \Xi) \|\nabla \boldsymbol{r}_{h}\|_{0}^{2}$$

$$\leq C(1 + \Xi) \left(\eta_{d} \|\operatorname{div} \boldsymbol{p}_{h}\|_{0}^{2} + \eta_{d} \|\boldsymbol{p}_{h}\|_{0}^{2} \right) \leq C(1 + \Xi) a_{d}(\boldsymbol{p}_{h}, \boldsymbol{p}_{h}), \tag{53}$$

where $\Xi = \max_{1 \leq i \leq N} (H_i/\delta_i)$.

In addition, the argument in (35) gives

$$F_{3,2} = C\eta_{d} \sum_{i=1}^{N} \sum_{j \in I_{i}} \sum_{K \in \mathcal{T}_{H}, \atop K \subset \overline{\Omega}_{j}} \frac{1}{\delta_{i} H_{i}} \|\boldsymbol{q}_{2}\|_{0,\Omega_{i}}^{2} \leqslant C\eta_{d} \Xi H^{-2} \|\boldsymbol{Q}_{H}^{\mathcal{R}\mathcal{T}} \boldsymbol{r}_{h} - \boldsymbol{r}_{h}\|_{0}^{2}$$

$$\leqslant C\eta_{d} \Xi \|\nabla \boldsymbol{r}_{h}\|_{0}^{2} \leqslant C\Xi \left(\eta_{d} \|\operatorname{div} \boldsymbol{p}_{h}\|_{0}^{2} + \eta_{d} \|\boldsymbol{p}_{h}\|_{0}^{2}\right)$$

$$\leqslant C\Xi a_{d}(\boldsymbol{p}_{h}, \boldsymbol{p}_{h}). \tag{54}$$

We therefore have the following inequality by using (48), (49), (50), (51), (53), and (54):

$$\sum_{i=1}^{N} \eta_d \|\operatorname{div} \boldsymbol{r}_i\|_{0,\Omega_i'}^2 \leqslant C \max_{1 \leqslant i \leqslant N} \left(1 + \frac{H_i}{\delta_i}\right) a_d(\boldsymbol{p}_h, \boldsymbol{p}_h). \tag{55}$$

Due to (47) and (55), we finally have

$$\sum_{i=1}^{N} a_d(\boldsymbol{r}_i, \boldsymbol{r}_i) \leq C \max_{1 \leq i \leq N} \left(1 + \frac{H_i}{\delta_i} \right) a_d(\boldsymbol{p}_h, \boldsymbol{p}_h).$$

Proposition 6. Assume that $\eta_d \leq 1$. Then, the term \widetilde{p}_i introduced in (43) has the following estimate:

$$\sum_{i=1}^{N} a_{d}(\widetilde{\boldsymbol{p}}_{i}, \widetilde{\boldsymbol{p}}_{i}) \leq Ca_{d}(\boldsymbol{p}_{h}, \boldsymbol{p}_{h}),$$

where the constant C is independent from N, h, H_i , δ_i , and η_d .

Proof. By using Lemma 3, the construction of the partition of unity set $\{\theta_i\}$ in (8), and (20), we obtain

$$\sum_{i=1}^{N} \|\widetilde{\boldsymbol{p}}_{i}\|_{0,\Omega_{i}'}^{2} \leq C \sum_{i=1}^{N} \|\theta_{i}\widetilde{\boldsymbol{p}}_{h}\|_{0,\Omega_{i}'}^{2} \leq C \|\widetilde{\boldsymbol{p}}_{h}\|_{0}^{2} \leq C \|\boldsymbol{p}_{h}\|_{0}^{2}.$$

$$(56)$$

From (8), Lemma 3, the inverse inequality, and (21), we have

$$\eta_{d} \sum_{i=1}^{N} \left\| \operatorname{div} \widetilde{\boldsymbol{p}}_{i} \right\|_{0,\Omega_{i}'}^{2} \leq C \eta_{d} \sum_{i=1}^{N} \delta_{i}^{-2} \left\| \widetilde{\boldsymbol{p}}_{h} \right\|_{0,\Omega_{i}'}^{2} + C \eta_{d} \left\| \operatorname{div} \widetilde{\boldsymbol{p}}_{h} \right\|_{0}^{2} \leq C \eta_{d} h^{-2} \left\| \widetilde{\boldsymbol{p}}_{h} \right\|_{0}^{2} \\
\leq C \left(\eta_{d} \left\| \operatorname{div} \boldsymbol{p}_{h} \right\|_{0}^{2} + \eta_{d} \left\| \boldsymbol{p}_{h} \right\|_{0}^{2} \right) \leq C a_{d} (\boldsymbol{p}_{h}, \boldsymbol{p}_{h}). \tag{57}$$

We therefore have

$$\sum_{i=1}^{N} a_{d}(\widetilde{\boldsymbol{p}}_{i}, \widetilde{\boldsymbol{p}}_{i}) \leqslant Ca_{d}(\boldsymbol{p}_{h}, \boldsymbol{p}_{h}).$$

Lemma 13. Assume that the constant η_d in (4) is less than or equal to one. Then, we have the following estimate for the local components in (22):

$$\sum_{i=1}^{N} a_d(\boldsymbol{p}_i, \boldsymbol{p}_i) \leqslant C\left(\max_{1 \leqslant i \leqslant N} \left(1 + \frac{H_i}{\delta_i}\right)\right) a_d(\boldsymbol{p}_h, \boldsymbol{p}_h), \tag{58}$$

where the constant C does not depend on N, h, H_i , δ_i , and η_d .

Proof. Based on Propositions 4, 5, and 6, we have (58).

Finally, We obtain an estimate of the condition number for our H(div) model problem.

Theorem 2. Let $\eta_d \leq 1$. We then have the following estimate:

$$\varkappa \left(M_d^{-1} A_d \right) \leqslant C \max_{1 \leqslant i \leqslant N} \left(1 + \frac{H_i}{\delta_i} \right), \tag{59}$$

where the constant C does not depend on the mesh sizes, H_i , δ_i , η_d , and the number of subdomains but may depend on N_0 .

Proof. We obtain (59) by using Lemmas 8, 9, 12, and 13.

Corollary 2. If the second Betti number of the domain Ω , i.e., the number of connected components of $\partial\Omega$ minus one, is zero, we have (59) in Theorem 2 without the assumption $\eta_d \leq 1$.

Proof. Provided that the second Betti number of the domain Ω is zero, we can replace the upper bound of (21) by simply the divergence term. We therefore remove the assumption regarding the coefficient η_d in Theorem 2; see [22, Sect. 5.2] for more detail.

5 Numerical experiments

In this section, we perform one experiment on an H(div) problem and four numerical experiments for H(curl)problems. We report the error profile associated with the following notations:

$$\begin{split} & \text{Error D1} := \|\Pi_h^{\mathcal{RT}} \boldsymbol{u} - \boldsymbol{u}_h\|_0, \\ & \text{Error D2} := \|\text{div} \Big(\Pi_h^{\mathcal{RT}} \boldsymbol{u} - \boldsymbol{u}_h\Big)\|_0, \\ & \text{Error 1} := \|\Pi_h^{\mathcal{ND}} \boldsymbol{u} - \boldsymbol{u}_h\|_0, \\ & \text{Error 2} := \|\text{curl} \Big(\Pi_h^{\mathcal{ND}} \boldsymbol{u} - \boldsymbol{u}_h\Big)\|_0 \quad \text{for 2D or } \|\text{curl} \Big(\Pi_h^{\mathcal{ND}} \boldsymbol{u} - \boldsymbol{u}_h\Big)\|_0 \quad \text{for 3D.} \end{split}$$

We also denote the number of iterations as follows.

 $I_1 :=$ Number of the conjugate gradient iterations,

 I_2 := Number of the domain – decomposition preconditioned conjugate gradient iterations.

In this work, we proved that

$$C_{\text{low}} \frac{a_c(\boldsymbol{u}_h, \boldsymbol{u}_h)}{(1 + H/\delta)} \leq a_c(M_c^{-1} A_c \boldsymbol{u}_h, \boldsymbol{u}_h) \leq C_{\text{high}} a_c(\boldsymbol{u}_h, \boldsymbol{u}_h)$$

$$(60)$$

for some positive constants \mathcal{C}_{low} and $\mathcal{C}_{\text{high}}$ independent of h, δ , and H. We also report the constants \mathcal{C}_{low} and $\mathcal{C}_{\text{high}}$ obtained numerically in each example. For each h, i.e., on each mesh \mathcal{T}_h , they are computed by

$$C_{\text{high}} = \lambda_{\text{max}}(M), \ C_{\text{low}} = \left(1 + \frac{H}{\delta}\right) \lambda_{\text{min}}(M), \ M = \sum_{i=0}^{N} R_c^{(i)} A_c^{(i)-1} R_c^{(i)} A_c,$$
 (61)

where λ_{\max} and λ_{\min} are the maximum eigenvalue and the minimum eigenvalue respectively, A_c is the stiffness matrix on \mathcal{T}_h , $A_c^{(0)}$ is the stiffness matrix on \mathcal{T}_H , $A_c^{(i)}$ is the stiffness matrix on subdomain $\mathcal{T}_h \cap \Omega_h^i$ for i > 0, and $R_c^{(i)}$ is the transfer matrix embedding the subspace functions to the fine space. For H(div) problems, we replace the index *c* by *d* in the above notations.

5.1 Raviart-Thomas rectangular element

We solve the following grad div equations on two domains:

grad div
$$\mathbf{u}_h + \mathbf{u}_h = \mathbf{f}$$
 in Ω ,
$$\mathbf{u}_h \cdot \mathbf{n} = g$$
 on $\partial \Omega$, (62)

where n is the unit outer normal vector, and

$$\Omega = (-1,1)^2 \setminus [0,1) \times (-1,0], \tag{63}$$

$$\Omega = (0,1)^2 \setminus [1/4, 3/4]^2. \tag{64}$$

In both cases, the exact solution of (66) is chosen as

$$\boldsymbol{u} = \begin{pmatrix} y^5 \\ x^4 \end{pmatrix}. \tag{65}$$

In both cases, the meshes used in the computation are uniform square meshes, as shown in Figure 1. For Ω in (63), we have three subdomains, i.e., on Grid 1, $\mathcal{T}_H = \{\Omega_i\}$, where

$$\Omega_i = \{ \text{a size} - 1 \text{ square} \}, \quad i = 1, 2, 3,$$

$$\Omega_i' = \Omega_i \cup \left(\bigcup_{K \in T_h, \atop \operatorname{dist}(K, \Omega) \leqslant h} K \right), \quad i = 1, 2, 3.$$

Thus, on Grid 1, all three $\Omega_i' = \Omega$. On a higher Grid \mathcal{T}_h , Ω_i' is the union of the square Ω_i and all size-h squares along its edges. For Ω in (64), we have 12 subdomains, i.e., on Grid 1, $\mathcal{T}_H = \{\Omega_i\}$, where

$$\Omega_i = \left\{ \text{a size} - \frac{1}{2} \text{ square} \right\}, \quad i = 1, \dots, 12,$$

$$\Omega_i' = \Omega_i \cup \left(\bigcup_{K \in \mathcal{T}_h. \atop \operatorname{dist}(K,\Omega) \leqslant h} K \right), \quad i = 1, \ldots, 12.$$

On a high Grid \mathcal{T}_h , Ω_i' is again the union of the square Ω_i and all size-h squares along its edges.

The results for computing (62) are listed in Table 1, where we can see that the finite element solution converges at the optimal order in both norms on both domains. Additionally, we can see that the condition number of domain-decomposition preconditioned system is roughly (1 + H/δ).

We list the computer found constants of (60) in Table 2. As proved in the theory, the constants remain bounded on the both non-convex domains.



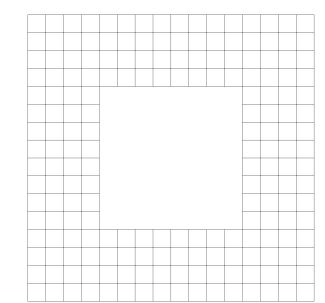


Figure 1: The third level grids for domain $\Omega =$ $(-1,1)^2\setminus[0,1)\times(-1,0]$ and $(0,1)^2\setminus[1/4,3/4]^2$, respectively.

Table 1: Error profile for (65) on grids as shown in Figure 1.

Grid	Error D1	Order	Error D2	Order	I_1	I_2
			On $\Omega = (-1,1)^2 \setminus [0,1)$	× (-1, 0]		
1	0.7610E+00	0.0	0.1080E+01	0.0	5	1
2	0.2561E+00	1.6	0.5896E+00	0.9	36	14
3	0.6919E-01	1.9	0.1633E+00	1.9	154	17
4	0.1763E-01	2.0	0.4180E-01	2.0	487	20
5	0.4428E-02	2.0	0.1051E-01	2.0	1,094	24
6	0.1108E-02	2.0	0.2631E-02	2.0	2,291	29
			On $\Omega = (0,1)^2 \setminus [1/4,3]$	B/4] ²		
1	0.3415E-01	0.0	0.7809E-01	0.0	16	5
2	0.8634E-02	2.0	0.2013E-01	2.0	125	21
3	0.2161E-02	2.0	0.5075E-02	2.0	530	23
4	0.5401E-03	2.0	0.1272E-02	2.0	1,298	27
5	0.1350E-03	2.0	0.3181E-03	2.0	2,708	32
6	0.3374E-04	2.0	0.7955E-04	2.0	5,610	40

Table 2: The bounds for 3-subdomain and for 12-subdomain overlap DD shown as in Figure 1.

Grid	C _{low} in (60)	C _{high} in (60)	C _{low} in (60)	C _{high} in (60)	
	On (−1,1) ² \[$(0,1)\times(-1,0]$	On (0,1) ² \[1/4,3/4] ²		
2	1.976790	3.429921	1.889383	3.492440	
3	2.358270	3.119507	2.120117	3.140896	
4	2.505871	3.025601	2.261999	3.030765	
5	2.555174	3.005602	2.337076	3.006730	
6	2.574040	3.001300	2.373954	3.001561	

Table 3: Effects of varying H, h, and δ for (62) on domain (63), on $\lambda_{\max}(M)$ and $\lambda_{\min}(M)$ in (61).

Η/δ	Н	δ	$\delta \qquad \qquad h = 2^{-2}$		$h = 2^{-3}$		$h = 2^{-4}$		$h = 2^{-5}$	
			λ_{max}	λ_{min}	λ_{max}	λ_{min}	λ_{max}	λ_{min}	$\lambda_{\sf max}$	λ_{min}
4	2 ⁰	2-2	3.119	0.988	3.107	0.562	3.064	0.651	3.064	0.593
	2-1	2-3	-	_	4.266	0.789	4.194	0.520	4.170	0.648
	2-2	2-4	-	_	_	_	4.413	0.772	4.280	0.501
	2-3	2-5	-	_	_	_	_	_	4.465	0.768
8	20	2-3	-	_	3.025	0.501	3.022	0.318	3.013	0.396
	2-1	2-4	-	_	_	_	4.078	0.499	4.046	0.294
	2-2	2-5	-	_	_	_	_	_	4.132	0.495
16	2^{0}	2-4	-	_	_	_	3.005	0.283	3.004	0.168
	2-1	2-5	-	_	-	_	-	-	4.020	0.284
32	2^0	2-5	-	-	-	-	-	-	3.001	0.151

Next, we examine the impact of varying the parameters H, h, and δ . This experiment is conducted using the computational domain defined in (63) and the initial grid shown in the left of Figure 1. We obtain finer grid using uniform refinements. We then apply our domain decomposition preconditioners using suitable combinations of H, h, and δ for each grid. The maximum and the minimum eigenvalues of M, introduced in (61), are presented in Table 3. The results show that the maximum eigenvalues remain close to 3 for the coarsest subdomain grid and around 4 for the finer grids. Additionally, we observe that the minimum eigenvalues decrease as the ratio H/δ increases.

5.2 Nédélec type-1 rectangular element

We solve the following **curl** curl equations on two domains:

curl curl
$$u_h + u_h = f$$
 in Ω ,
 $u_h \times n = g$ on $\partial \Omega$, (66)

where n is the unit outer normal vector, and

$$\Omega = (0,1)^2 \setminus (([1/4,1/2] \times [1/4,1/2]) \cup ([1/2,3/4] \times [1/2,3/4]), \tag{67}$$

$$\Omega = (0,1)^2 \setminus (([1/4,1) \times [3/4,1) \cup ([1/4,1) \times [1/4,1/2]).$$
(68)

In both cases, the exact solution of (66) is chosen as

$$\boldsymbol{u} = \begin{pmatrix} x^2 y^2 \\ x^2 y^3 \end{pmatrix}. \tag{69}$$

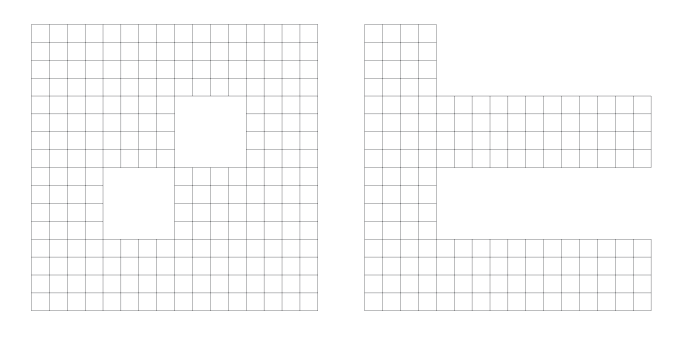


Figure 2: The third level grids for domains Ω in (67) (with 14 size- $\frac{1}{4}$ square subdomains Ω_i) and (70) (with 8 size- $\frac{1}{4}$ square subdomains Ω_i), respectively.

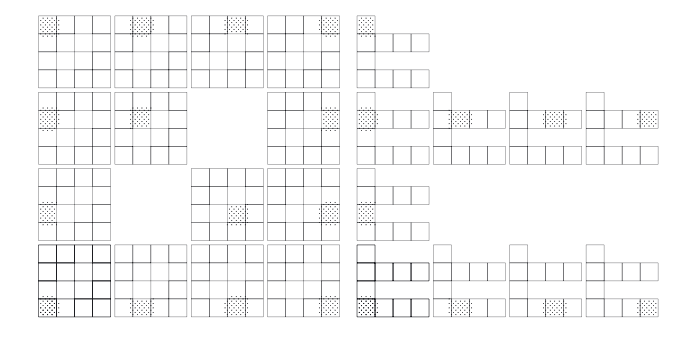


Figure 3: Left: The level three function nodes in 14 subdomains; Right: The 8 subdomain nodes.

In both cases, we use nested refinement square meshes, as shown in Figure 2.

We show the minimum overlapping domain decomposition by Figure 3, where the third-level finite element nodes are plotted for each subdomain.

The results are listed in Table 4, where we can see that the finite element solution converges at the optimal order in both norms on both domains.

We list the computer found constants of (62) in Table 5. As proved in the theory, the constants are apparently bounded above (C_{high}) and below (C_{low}) . But they seem to depend on the domain.

Table 4: Error profile for (69) on grids as shown in Figure 2.

Grid	Error 1	Order	Error 2	Order	I_1	I_2
			On Ω in (67)			
1	0.1697E-01	0.0	0.1150E-01	0.0	42	14
2	0.4376E-02	2.0	0.2962E-02	2.0	244	25
3	0.1103E-02	2.0	0.7465E-03	2.0	758	28
4	0.2764E-03	2.0	0.1870E-03	2.0	1,701	32
5	0.6915E-04	2.0	0.4680E-04	2.0	3,467	38
6	0.1729E-04	2.0	0.1170E-04	2.0	6,979	45
			On Ω in (68)			
1	0.1071E-02	0.0	0.1854E-02	0.0	20	9
2	0.1196E-02	0.0	0.7785E-03	1.3	159	23
3	0.3336E-03	1.8	0.2102E-03	1.9	636	25
4	0.8557E-04	2.0	0.5354E-04	2.0	1,447	27
5	0.2154E-04	2.0	0.1345E-04	2.0	3,027	33
6	0.5395E-05	2.0	0.3368E-05	2.0	6,159	40

Table 5: The bounds for small-overlap DD shown as in Figure 3.

Grid	C _{low} in (60)	C _{high} in (60)	C _{low} in (60)	C _{high} in (60)	
	On Ω	in (69)	On Ω in (70)		
2	1.883353	4.488207	1.976790	3.429921	
3	2.083264	4.163713	2.358270	3.119507	
4	2.221202	4.045254	2.505871	3.025601	
5	2.296535	4.011663	2.555174	3.005602	

5.3 Nédélec type-1 rectangular element again

We solve equations (66) again on

$$\Omega = (0,1)^2$$
 or $(0,1)^2 \setminus \{1/2\} \times (0,1/2]$.

In both cases, the exact solution of (66) is chosen as

$$\boldsymbol{u} = \begin{pmatrix} y^5 \\ \chi^4 \end{pmatrix}. \tag{70}$$

In both cases, the meshes used in the computation are uniform square meshes, as shown in Figure 4. The results are listed in Table 6, where we can see that the finite element solution converges at the optimal order in both norms on both domains.

In this example, we subdivide both Ω into four subdomains, as shown in Figure 5. We consider a minimum overlapping domain decomposition. We plot the nodes of the third-level finite element function inside each subdomain. We note that the horizontal nodes belong to the first component of the vector H(curl) function. The difference between the graphs is at the nodes on the lower middle vertical edge, which is a boundary edge.

We list the computer found constants of (60) in Table 7. As proved in the theory, the constants remain bounded when doing domain decomposition methods on the non-convex domain $\Omega = (0, 1)^2 \setminus \{1/2\} \times (0, 1/2]$.

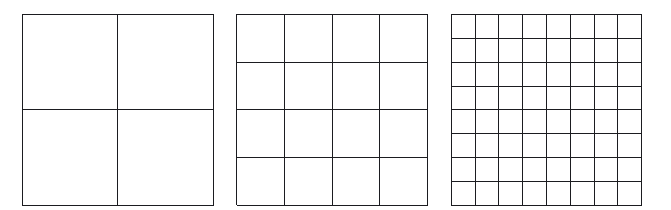


Figure 4: The first three grids on $\Omega = (0,1)^2$ (with 4 size- $\frac{1}{2}$ square subdomains Ω_i) for computing Tables 6–7.

Table 6: Error profile for (70) on grids as shown in Figure 4.

Grid	Error 1	Order	Error 2	Order	Error 1	Order	Error 2	Order
		On Ω =	= (0,1) ²			On $\Omega = (0,1)$	² \{1/2} × (0, 1/2]	
1	8.97E-2	0.0	3.11E-1	0.0	1.27E-1	0.0	2.77E-1	0.0
2	2.67E-2	1.7	8.80E-2	1.8	3.36E-2	1.9	8.19E-2	1.8
3	6.94E-3	1.9	2.26E-2	2.0	8.49E-3	2.0	2.13E-2	1.9
4	1.75E-3	2.0	5.69E-3	2.0	2.12E-3	2.0	5.37E-3	2.0
5	4.39E-4	2.0	1.43E-3	2.0	5.29E-4	2.0	1.35E-3	2.0
6	1.10E-4	2.0	3.56E-4	2.0	1.32E-4	2.0	3.37E-4	2.0
7	2.75E-5	2.0	8.91E-5	2.0	3.30E-5	2.0	8.43E-5	2.0
8	6.87E-6	2.0	2.23E-5	2.0	8.24E-6	2.0	2.11E-5	2.0

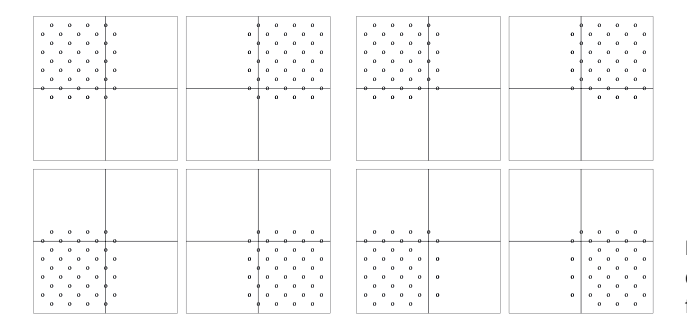


Figure 5: Left: The level three function nodes in the four subdomains, where $\Omega = (0, 1)^2$; Right: The 4-subdomain nodes for $\Omega = (0,1)^2 \setminus \{1/2\} \times (0,1/2]$.

Table 7: The bounds for 4-subdomain small-overlap DD shown as in Figure 5.

Grid	C _{low} in (60)	C _{high} in (60)	C _{low} in (60)	C _{high} in (60)		
	On Ω :	= (0,1) ²	On $\Omega = (0,1)^2 \setminus \{1/2\} \times (0,1/2]$			
2	2.015473	4.485408	1.958618	4.349539		
3	2.553089	4.162126	2.271621	4.092826		
4	2.843341	4.044754	2.414993	4.022131		
5	2.999805	4.011540	2.463830	4.005278		
6	3.088654	4.002915	2.477246	4.001282		

5.4 Triangular Nédélec element

We solve the **curl** curl equation (66) again on two domains

$$\Omega = (0,1)^2$$
 or $(0,1)^2 \setminus \{1/2\} \times (0,1/2]$.

The exact solution of (66) is chosen as

$$\boldsymbol{u} = \begin{pmatrix} x^2 y^2 \\ x^2 y \end{pmatrix}. \tag{71}$$

In both cases, the meshes used in the computation are uniform triangular meshes, as shown in Figure 6. The results are listed in Table 8, where we can see that the finite element solution converges at the optimal order in both norms on both domains.

Again we do iterations based on domain decomposition methods with four subdomains for both domains Ω , as shown in Figure 7. We plot the nodes of the third-level finite element function inside each subdomain, in Figure 7. The difference between two graphs is at the nodes on the lower middle vertical edge, which is a boundary edge.

We list the computer found constants of (60) in Table 9. As proved in the theory, the constants remain bounded on the non-convex domain $\Omega = (0,1)^2 \setminus \{1/2\} \times (0,1/2]$, in Table 9.

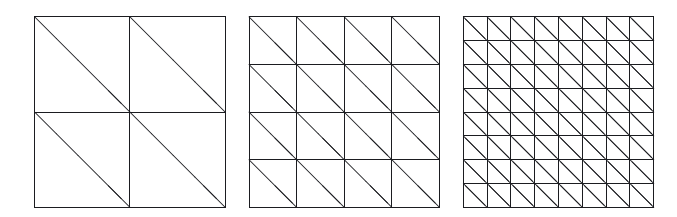


Figure 6: The first three grids on $\Omega = (0,1)^2$ (with 4 size- $\frac{1}{2}$ square subdomains Ω_i) for the computation Tables 8–9.

Table 8: Error profile for (71) on grids as shown in Figure 6.

Grid	Error 1	Order	Error 2	Order	Error 1	Order	Error 2	Order
		On Ω :	= (0,1) ²			On $\Omega=$ (0,1)	² \{1/2} × (0, 1/2]	
1	1.17E-2	0.0	7.19E-2	0.0	1.19E-2	0.0	7.18E-2	0.0
2	3.19E-3	1.9	4.00E-2	0.8	3.29E-3	1.9	4.00E-2	0.8
3	8.12E-4	2.0	2.05E-2	1.0	8.35E-4	2.0	2.05E-2	1.0
4	2.04E-4	2.0	1.03E-2	1.0	2.10E-4	2.0	1.03E-2	1.0
5	5.10E-5	2.0	5.15E-3	1.0	5.24E-5	2.0	5.15E-3	1.0
6	1.27E-5	2.0	2.58E-3	1.0	1.31E-5	2.0	2.58E-3	1.0
7	3.19E-6	2.0	1.29E-3	1.0	3.28E-6	2.0	1.29E-3	1.0
8	7.97E-7	2.0	6.44E-4	1.0	8.19E-7	2.0	6.44E-4	1.0

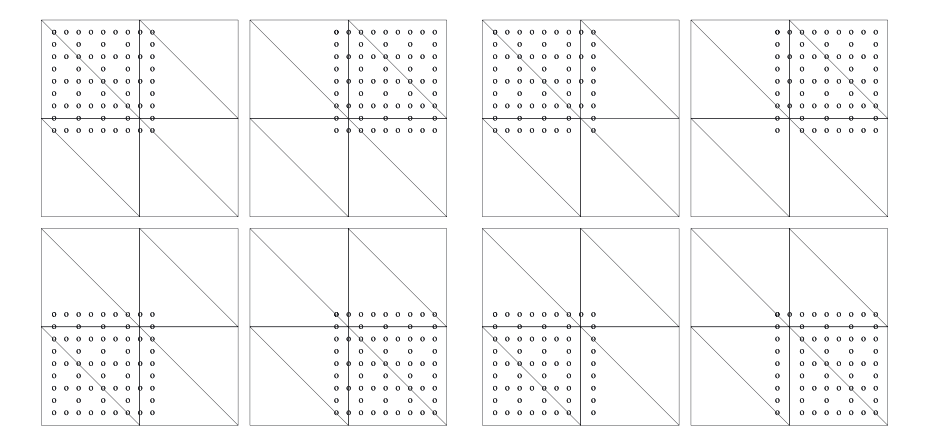


Figure 7: Left: The level three function nodes in the four subdomains, where $\Omega = (0,1)^2$; Right: The 4-subdomain nodes for $\Omega = (0,1)^2 \setminus \{1/2\} \times (0,1/2]$.

Table 9: The bounds for 4-subdomain small-overlap DD shown as in Figure 7.

Grid	C _{low} in (60)	C _{high} in (60)	C _{low} in (60)	C _{high} in (60)		
	On Ω :	$=(0,1)^2$	On $\Omega = (0,1)^2 \setminus \{1/2\} \times (0,1/2]$			
2	3.575004	5.000000	3.628239	5.000000		
3	2.609161	4.614568	2.641507	4.611478		
4	3.750690	4.192807	3.381828	4.191696		
5	4.932503	4.049440	4.015695	4.049120		
6	5.554555	4.012045	4.459404	4.011962		

5.5 Tetrahedral Nédélec element

We solve the equation

curl curl
$$u_h + u_h = f$$
 in Ω ,
 $u_h \times n = g$ on $\partial \Omega$,
$$(72)$$

on two 3D domains

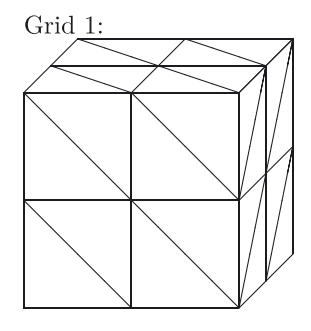
$$\Omega = (0,2)^3$$
 or $(0,2)^3 \setminus \{1\} \times [1,2)^2$.

The exact solution of (72) is chosen as

$$\boldsymbol{u} = \begin{pmatrix} x^2 \\ x^2 \\ y^2 \end{pmatrix}. \tag{73}$$

In both cases, the meshes used in the computation are uniform tetrahedral meshes, as shown in Figure 8. The results are listed in Table 10, where we can see that the finite element solution converges at the optimal order in both norms on both domains.

We perform domain decomposition iterations with eight subdomains for both domains of a cube and a cube with a cut. The eight subdomains are the eight unit cubes in the left graph of Figure 8. We list the computer found constants of (60) in Table 11. As proved in the theory, the constants remain bounded on the non-convex domain $\Omega = (0,2)^3 \setminus \{1\} \times [1,2)^2$, in Table 11. It seems the C_{low} in Table 11 may keep growing. It would break the theory only when C_{low} decreases to 0. We note again that we improved previous theoretic lower bound from $O((1+H/\delta)^2)$ to $O(1+H/\delta)$. The $C_{\rm low}$ in the 2D examples seems to confirm that $O(1+H/\delta)$ is the optimal lower bound. But we are not sure if the computation is done on high enough levels to enter the asymptotic range, or if the lower bound $O(1 + H/\delta)$ can be further improved in theory for 3D tetrahedral edge elements.



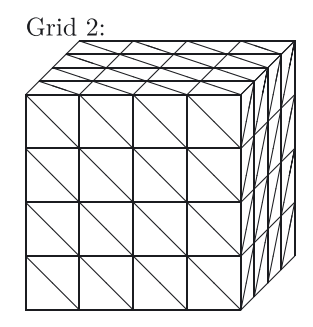


Figure 8: The first two grids on $\Omega = (0, 2)^3$ (with 8 size-1 cube subdomains Ω_i) for the computation in Tables 10–11.

Table 10: Error profile for (73) on grids as shown in Figure 8.

Grid	Error 1	Order	Error 2	Order	Error 1	Order	Error 2	Order
	On $\Omega = (0,2)^3$					On $\Omega = (0,$	$2)^3\backslash\{1\}\times[1,2)^2$	
1	8.24E-2	0.0	4.57E-1	0.0	8.53E-2	0.0	4.22E-1	0.0
2	2.82E-2	1.5	3.13E-1	0.5	2.82E-2	1.6	3.04E-1	0.5
3	7.75E-3	1.9	1.75E-1	0.8	7.75E-3	1.9	1.73E-1	0.8
4	2.01E-3	1.9	9.21E-2	0.9	2.01E-3	1.9	9.16E-2	0.9
5	5.09E-4	2.0	4.71E-2	1.0	5.10E-4	2.0	4.70E-2	1.0
6	1.28E-4	2.0	2.38E-2	1.0	1.29E-4	2.0	2.38E-2	1.0

Table 11: The bounds for 8-subdomain DD on meshes shown as in Figure 8.

Grid	C _{low} in (60)	C _{high} in (60)	C _{low} in (60)	C _{high} in (60)
	On Ω :	= (0,2) ³	$On \Omega = (0,2)$	$3\setminus\{1\}\times[1,2)^2$
1	1.525539	5.846509	1.662208	5.543800
2	1.792536	8.408068	1.815730	8.381018
3	2.845118	8.410624	2.856422	8.390277
4	4.741863	8.410624	4.760704	8.390277

5.6 Hexahedral Nédélec and Raviart-Thomas elements

Regarding experiments in this subsection, we solve (72) using hexahedral Nédélec elements and (62) using hexahedral Raviart-Thomas elements on the domain

$$\Omega = (-1, 1)^3 \setminus (-1, 0)^3. \tag{74}$$

In each experiment, we start with the computational grid (Grid 1) that has a uniform mesh size of h = 1/8, as shown in Figure 9. Grid 2 and Grid 3 are then generated through uniform refinement, resulting in mesh sizes of h = 1/16 and h = 1/32, respectively. On each grid, we apply overlapping Schwarz methods using 56 (H=1/2), 448 (H=1/4), and 3,584 (H=1/8) uniformly sized subdomains, with overlap widths $\delta=h$, 2h, and 4h selected as appropriate. We report $\lambda_{\max}(M)$ and $\lambda_{\min}(M)$ introduced in (62) in Table 12 and Table 13 for solving (72) and (62), respectively. For both cases, we observe that $\lambda_{\max}(M)$ remains approximately 8, while $\lambda_{\min}(M)$ decreases linearly on H/δ .

Remark 5. Across all experiments, we find that C_{high} , or equivalently $\lambda_{\text{max}}(M)$, is typlically around 4 for twodimensional problems and around 8 for three-dimensional problems. In some two-dimensional cases, C_{high} is close to 3. This value appears to be related to the maximum number of extended subdomains that intersect at

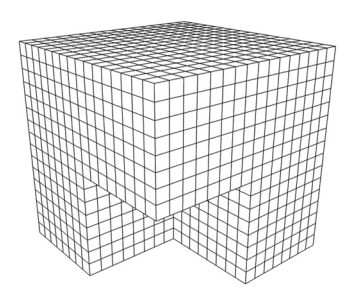


Figure 9: The first grid (Grid 1) on $\Omega = (-1, 1)^3 \setminus (-1, 0)^3$.

Table 12: Effects of varying H, h, and δ on $\lambda_{\max}(M)$ and $\lambda_{\min}(M)$ (hexahedral Nédélec element).

H/δ	Н	δ	Grid 1 ($h = 1/8$)		Grid 2 (/	h = 1/16)	Grid 3 ($h = 1/32$)	
			λ_{max}	λ_{min}	λ_{max}	λ_{min}	λ_{max}	λ_{min}
4	1/2	1/8	8.148544	0.827472	8.144804	0.814285	8.145592	0.811781
	1/4	1/16	_	_	8.217663	0.800833	8.221615	0.784011
	1/8	1/32	_	_	_	_	8.239654	0.792617
8	1/2	1/16	_	_	8.021819	0.499111	8.019272	0.496113
	1/4	1/32	_	_	_	-	8.033401	0.446827
16	1/2	1/32	_	_	_	_	8.002735	0.269601

Table 13: Effects of varying H, h, and δ on $\lambda_{\max}(M)$ and $\lambda_{\min}(M)$ (hexahedral Raviart–Thomas element).

Н/δ	Н	δ	Grid 1 (h = 1/8)		Grid 2 (h = 1/16)		Grid 3 ($h = 1/32$)	
			λ_{max}	λ_{min}	λ_{max}	λ_{min}	λ_{max}	λ_{min}
4	1/2	1/8	8.098781	0.952532	8.097748	0.946058	8.098756	0.944307
	1/4	1/16	_	_	8.132513	0.937809	8.127692	0.932332
	1/8	1/32	_	_	_	_	8.129632	0.929873
8	1/2	1/16	_	_	8.004314	0.690814	8.004023	0.686388
	1/4	1/32	_	_	_	_	8.000589	0.661720
16	1/2	1/32	_	_	_	_	8.000311	0.394069

a single point. In ideal scenarios with regularly shaped domains and subdomains (such as cubes), the expected values are 4 in two dimensions and 8 in three dimensions. However, when the domain or subdomains are irregularly shaped, these values may vary, as reflected in our experimental results.

Acknowledgments: The authors are grateful to reviewers for their valuable comments and suggestions, which helped to enhance the quality of this manuscript.

Research ethics: Not applicable. **Informed consent:** Not applicable.

Author contributions: All authors have accepted responsibility for the entire content of this manuscript and approved its submission.

Use of Large Language Models, AI and Machine Learning Tools: In writing, we used DeepL to check spelling and grammar issues.

Conflict of interest: The authors state no conflict of interest.

Research funding: D.-S. Oh was supported in part by Basic Science Research Program through the National Research Foundation of Korea (NRF) funded by the Ministry of Education (No. RS-2023-00244515) and by the Korea government (MSIT) (No. 2020R1F1A1A01072168).

Data availability: Not applicable.

References

- [1] A. Bossavit, "Discretization of electromagnetic problems: the "generalized finite differences" approach," in Handbook of Numerical Analysis, vol. XIII, North-Holland, Amsterdam, 2005, pp. 105-197.
- [2] P. B. Monk, "A mixed method for approximating Maxwell's equations," SIAM J. Numer. Anal., vol. 28, no. 6, pp. 1610 1634, 1991.
- [3] Z. Cai, R. Lazarov, T. A. Manteuffel, and S. F. McCormick, "First-order system least squares for second-order partial differential equations. I," SIAM J. Numer. Anal., vol. 31, no. 6, pp. 1785-1799, 1994.
- [4] Z. Cai, C. Tong, P. S. Vassilevski, and C. Wang, "Mixed finite element methods for incompressible flow: stationary Stokes equations," Numer. Methods Part. Differ. Equ., vol. 26, no. 4, pp. 957-978, 2010.
- [5] P. Lin, "A sequential regularization method for time-dependent incompressible Navier-Stokes equations," SIAM J. Numer. Anal., vol. 34, no. 3, pp. 1051-1071, 1997.
- [6] J. G. Calvo, "A new coarse space for overlapping Schwarz algorithms for H(curl) problems in three dimensions with irregular subdomains," Numer. Algorithms, vol. 83, no. 3, pp. 885 – 899, 2020.
- [7] R. Hiptmair and A. Toselli, "Overlapping and multilevel Schwarz methods for vector valued elliptic problems in three dimensions," in Parallel solution of partial differential equations (Minneapolis, MN, 1997), ser. IMA Vol. Math. Appl., vol. 120, New York, Springer, 2000, pp. 181-208.
- [8] Q. Liang, X. Xu, and S. Zhang, "On a sharp estimate of overlapping Schwarz methods in H(curl; Ω) and H(div; Ω)," *IMA J. Numer.* Anal., vol. 45, no. 2, pp. 1009-1027, 2025.
- [9] A. Toselli, "Overlapping Schwarz methods for Maxwell's equations in three dimensions," Numer. Math., vol. 86, no. 4, pp. 733 752,
- [10] C. R. Dohrmann and O. B. Widlund, "A BDDC algorithm with deluxe scaling for three-dimensional H(curl) problems," Comm. Pure Appl. Math., vol. 69, no. 4, pp. 745-770, 2016.
- [11] A. Toselli, "Domain decomposition methods of dual-primal FETI type for edge element approximations in three dimensions," C. R. Math. Acad. Sci. Paris, vol. 339, no. 9, pp. 673-678, 2004.
- [12] S. Zampini, "Adaptive BDDC deluxe methods for H(curl)," in Domain Decomposition Methods in Science and Engineering, XXIII, ser. Lect. Notes Comput. Sci. Eng., vol. 116, Cham, Springer, 2017, pp. 285-292.
- [13] D. N. Arnold, R. S. Falk, and R. Winther, "Preconditioning in H(div) and applications," Math. Comp., vol. 66, no. 219, pp. 957–984, 1997.
- [14] D.-S. Oh, "An overlapping Schwarz algorithm for Raviart-Thomas vector fields with discontinuous coefficients," SIAM J. Numer. Anal., vol. 51, no. 1, pp. 297-321, 2013.
- [15] D.-S. Oh, O. B. Widlund, S. Zampini, and C. R. Dohrmann, "BDDC algorithms with deluxe scaling and adaptive selection of primal constraints for Raviart-Thomas vector fields," Math. Comp., vol. 87, no. 310, pp. 659 – 692, 2018.
- [16] B. I. Wohlmuth, A. Toselli, and O. B. Widlund, "An iterative substructuring method for Raviart-Thomas vector fields in three dimensions," SIAM J. Numer. Anal., vol. 37, no. 5, pp. 1657 – 1676, 2000.
- [17] J. Xu, "Iterative methods by space decomposition and subspace correction," SIAM Rev., vol. 34, no. 4, pp. 581 613, 1992.

- [18] M. Dryja and O. B. Widlund, "Domain decomposition algorithms with small overlap," SIAM J. Sci. Comput., vol. 15, no. 3, pp. 604-620, 1994.
- [19] A. Toselli and O. Widlund, Domain decomposition methods algorithms and theory, ser. Springer Series in Computational Mathematics, vol. 34, Berlin, Springer-Verlag, 2005.
- [20] S. C. Brenner, "Lower bounds for two-level additive Schwarz preconditioners with small overlap," SIAM J. Sci. Comput., vol. 21, no. 5, pp. 1657 – 1669, 2000, iterative methods for solving systems of algebraic equations (Copper Mountain, CO, 1998). https://doi.org/ 10.1137/S1064827598336483.
- [21] R. Hiptmair and J. Xu, "Nodal auxiliary space preconditioning in H(curl) and H(div) spaces," SIAM J. Numer. Anal., vol. 45, no. 6, pp. 2483-2509, 2007.
- [22] R. Hiptmair and C. Pechstein, "Regular decompositions of vector fields continuous, discrete, and structure-preserving," 2019. [Online]. Available at: https://www.sam.math.ethz.ch/sam_reports/reports_final/reports2019/2019-18.pdf.
- [23] R. Hiptmair and C. Pechstein, "Discrete regular decompositions of tetrahedral discrete 1-forms," in Maxwell's equations—analysis and numerics, ser. Radon Ser. Comput. Appl. Math., vol. 24, Berlin, De Gruyter, 2019, pp. 199-258.
- [24] R. Hiptmair and C. Pechstein, "A review of regular decompositions of vector fields: continuous, discrete, and structure-preserving," in Spectral and high order methods for partial differential equations — ICOSAHOM 2018, ser. Lect. Notes Comput. Sci. Eng., vol. 134, Cham, Springer, 2020, pp. 45-60.
- [25] R. S. Falk and R. Winther, "Local bounded cochain projections," Math. Comp., vol. 83, no. 290, pp. 2631 2656, 2014.
- [26] L. R. Scott and S. Zhang, "Finite element interpolation of nonsmooth functions satisfying boundary conditions," Math. Comp., vol. 54, no. 190, pp. 483-493, 1990.
- [27] A. Toselli, Domain decomposition methods for vector field problems, Ann Arbor, MI, ProQuest LLC, 1999, Ph.D. thesis, New York University. [Online]. Available at: https://cs.nyu.edu/media/publications/TR1999-785.pdf.